2017-01-01

Design & Analysis of a 500 lbf Liquid Oxygen and Liquid Methane Rocket Engine

Daniel Eduardo Vargas
University of Texas at El Paso, devargasfranco@miners.utep.edu

DESIGN & ANALYSIS OF A 500 LBF LIQUID OXYGEN AND LIQUID METHANE ROCKET ENGINE

DANIEL VARGAS FRANCO

Master's Program in Mechanical Engineering

APPROVED:

Ahsan Choudhuri, Ph.D., Chair

Jack Chessa, Ph.D.

Luis Rene Contreras, Ph.D.

Charles H. Ambler, Ph.D.
Dean of the Graduate School

DESIGN & ANALYSIS OF A 500 LBF LIQUID OXYGEN AND LIQUID METHANE ROCKET ENGINE

by

DANIEL VARGAS FRANCO, B.S.ME

THESIS

Presented to the Faculty of the Graduate School of

The University of Texas at El Paso

in Partial Fulfillment

of the Requirements

for the Degree of

MASTER OF SCIENCE

Department of Mechanical Engineering

THE UNIVERSITY OF TEXAS AT EL PASO

December 2017

Acknowledgements

Foremost, I would like to express my gratitude to my advisor Dr. Ahsan Choudhuri for the useful comments, engagement, and continuous support of my Master's study and for giving me the opportunity to conduct research at the UTEP Center for Space Exploration and Technology Research (cSETR). I would also like to thank the other members of my committee, Dr. Chessa and Dr. Luis Rene Contreras for participating in the review of my research.

My sincere thanks to the National Aeronautics and Space Administration Johnson Space Center propulsion branch for your guidance, support, and willingness to help my research team on complex rocket engine topics that are invaluable for a successful engine design.

I would like to extend my gratitude to all the NASA mentors I had on my two internships. Thank you for giving me the opportunity to intern with NASA to gain invaluable experience and helping me grow as a professional. And finally, I would like to thank my friends and family, they're the reason I continue to strive for success in my life.

Abstract

The rapid growth in demand for spacecraft technologies has spawned a need for a variety of new and innovative research. The utilization of liquid oxygen (LOX) and liquid methane (LCH4) in rocket engines have played an important role in space exploration efforts to promote missions to Mars with in-situ resource utilization for propellant production. This will allow the production of fuel needed to come back to Earth making the overall mission more cost effective by enabling larger usable mass.

The Center for Space Exploration and Technology Research has focused its efforts to developing Liquid Oxygen (LOX) and Liquid Methane (LCH4) propulsion technologies. The goal is to design, build, and test a 500 lbf throattleable (4:1) liquid oxygen and liquid methane rocket engine. Many iterations of this engine were developed taking into consideration many variables that are present in the design of rocket engines such as combustion instabilities, oscillatory combustion, stress, pressure, and fatigue. This thesis describes the design process, analysis, and decision making behind the design changes of this engine and plans for future development. It will be designed, built, and tested by cSETR. The end goal of CROME is to be the main propulsion engine for Daedalus suborbital flight vehicle and fire in space to obtain performance data of this propellant combination.

Table of Contents

List of Tables

List of Figures

Chapter 1: Introduction

Liquid Oxygen (LOX) and Liquid Methane (LCH4) is the most promising rocket fuel towards the journey to Mars. In the past, other better performing propellant combinations have been employed in the aerospace industry, like Liquid Hydrogen and LOX. However, using LOX and LCH4 has a lot of benefits over traditional hydrogen and LOX launch systems. Hydrogen gives a higher specific impulse but all the modifications required to deal with hydrogen negate that gain. This is due to methane being denser which would require much smaller tanks making the overall design much lighter. Also, methane is more stable in space over long periods of time vs hydrogen/LOX and does not need highly insulated cryogenic tanks. Methane has a boiling point much closer to that of oxygen allowing a simple bulkhead design. Most importantly, it can be produced from local sources on Mars using in-situ resource utilization (ISRU) technology. This technology consists in the practice of leveraging resources found on other astronomical objects to fulfill the requirements to come back to Earth. Which would make the mission more affordable and it allows the mission to carry more payload instead of fuel weight.

This has led companies to develop their own liquid methane propulsion systems all with the same purpose of enabling the technology to explore Mars and other space entities. Some examples are the Space X Raptor engine and the Blue Origin BE-4 engine.

The UTEP Center of Space Exploration and Technology Research (cSERTR) in partnership with the National Aeronautics and Space Administration (NASA) has been leading research center for the advancement of LOX and LCH4 propulsion technologies. This paper discusses the design and analysis process used to develop the last version of Centennial Restartable Oxygen Methane Engine (CROME), a throattable 500 lbf LOX/LCH4 rocket engine. It will

include detailed description of the assumptions made and finite element analysis for each major component.

1.1 Background

The cSETR has focused its efforts in the use of methane as a propellant. Nowadays, space exploration is relatively new and sending anything to space requires lot of money and planning. Because of this, it would be beneficial to be able to use all the resources available in space. In-situ resource utilization (ISRU) technology can provide the propellant necessary to come back to Earth. ISRU can reduce the mass and cost of space exploration architectures, reducing the amount of payload that must be launched from Earth. It is well known, that there is water on Mars. So, propellant can be produced from the Martian surface using two chemical reactions, water electrolysis and the Sabatier Reaction.

The CROME engine will be the main propulsion system for DEADALUS. The cSETR DEADALUS project is based on NASA's Project Morpheus, which also utilized a pintle injector. This would become beneficial during the project since doubts and questions about design could be addressed to the NASA team in Johnson Space Center in Houston, TX. The end goal of the DEADALUS and CROME project is to successfully operate an integrated LOX/LCH_4 engine.

1.2 Green Propellants

The propellants used have large biological impacts. Ground-based impacts can vary from groundwater contamination to explosions caused by mishandling of propellants. Hypergolic propellants are among the most efficient rocket fuels we know but are highly toxic and unstable. Also, these propellants have high impact on the atmosphere generally caused by the interaction of

the propellant exhaust with the atmosphere; biological impacts tend to focus on the toxicology and corrosiveness of propellants. This is why we focused our research on liquid methane, it is easier to handle and does not ignite unless properly atomized and mixed with an oxidizer. LCH4 is suitable for ISRU and can lower the negative impact on our atmosphere. The term “green propellant” is often confused because many can assume it has no negative effect on the environment, this is almost physically impossible, any propellant affects the environment in some way.

Green propulsion will depend on its ability to satisfy the two main drivers for its development, performance and lower costs. Currently, the atmospheric impact remains low because launch rates remain low, but it is important to start limiting environmental effects in order to pursue more efficient interplanetary explorations.

1.3 Previous Work

Not only has NASA done work on LO2-LCH4 propulsion technologies but private companies like Blue Origin and SpaceX have also invested in them. The main objective for both companies is reusability. This is due to their desire of decreasing the cost to reach outer space. Their work includes the achievement of vertical propulsive landing. Blue Origin achieved this with New Shepard and Space X with Falcon 9. With this they got closer to their goal of reusability of space crafts. Also, the ability of generating the LO2-LCH4 fuel on the landing site will help the human missions of space exploration.

NASA has its own vehicle capable of vertical take-off and landing (VTOL) which is called Morpheus. This planetary lander was built with the purpose to test the autonomous landing and hazard avoidance and the integration of LO2-LCH4 propulsion (Hart & Devolites, 2014). This

craft allowed the successful demonstration of an autonomous and unmanned landing by picking a safe landing zone. Morpheus had three different levels of test at Kennedy Space Center (KSC). The first one was a hot-fire test which was performed to see the fire sequence initiated with the control software. After that one, tethered testing followed. The vehicle was suspended from a crane and its navigation and control systems helped it hover in midair. One of the tethered tests was unsuccessful but this helped to prepare the vehicle better. The final test was a free flight test. In 2012 on one of the free flight tests Morpheus lost communication and most of the vehicle was lost. A second Morpheus was built, but this time around the tethered flights were more extraneous. Then, it was able to land safely on the free flight missions.

Figure 1 Morpheus Main Engine Test

The main drivers of the Morpheus propulsion system developed by NASA was to produce a low cost vehicle. The first iteration of the Morpheus project used an engine called HD, designed to provide 2,700 lbf of thrust. This project has been used as a baseline for the DEADALUS project. Lessons learned and approach used by the team in charge of the Morpheus project helped the cSETR to define our engine. UTEP and JSC have a partnership and many NASA engineers gave us constant mentoring and shared the knowledge to benefit the development of our project. This thesis and project borrows the concepts and design features of the Morpheus and improves some of its aspects.

Chapter 2: CROME Development Purpose

The Centennial Restartable Oxygen Methane Engine (CROME) will be used as the main propulsion system for the DEADALUS vehicle. Both, vehicle and engine, were designed in parallel so many of the engine parameters and requirements are derived from DEADALUS.

2.1 Deadalus Vehicle Overview

DEADALUS is a suborbital demonstration vehicle and its goal is to evaluate performance under microgravity conditions incorporating methane propulsion technologies. The propulsion system includes the main engine and a reaction control engine (RCE), a derivative of previous work conducted both by NASA and cSETR, which is designed around being integrated within this vehicle. The RCEs are the secondary source of propulsion for this vehicle. Through the partnership with NASA, the cSETR was able to obtain the RCE CAD model used on the Morpheus vehicle. Upon this design modifications were made to improve performance.

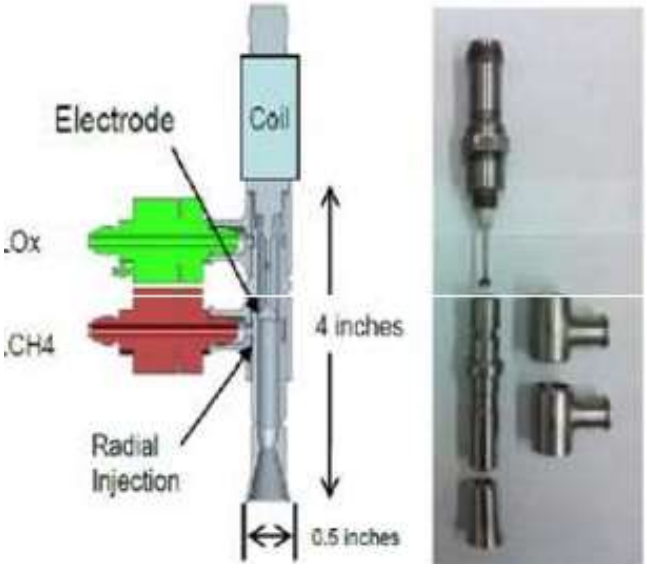

Figure 2 NASA Design of RCS

This RCE is capable of providing 5 lbf of thrust at sea level based on like-impinging elements going through the combustion chamber and then ignited using a spark plug. A module was designed to accommodate the RCEs, valves, and instrumentation.

The final stage vehicle will be launched via first stage sounding rocket where it will remain in sub-orbit at 90 miles above sea level around 200 seconds, as shown in Figure 3, while sending performance data back to earth.

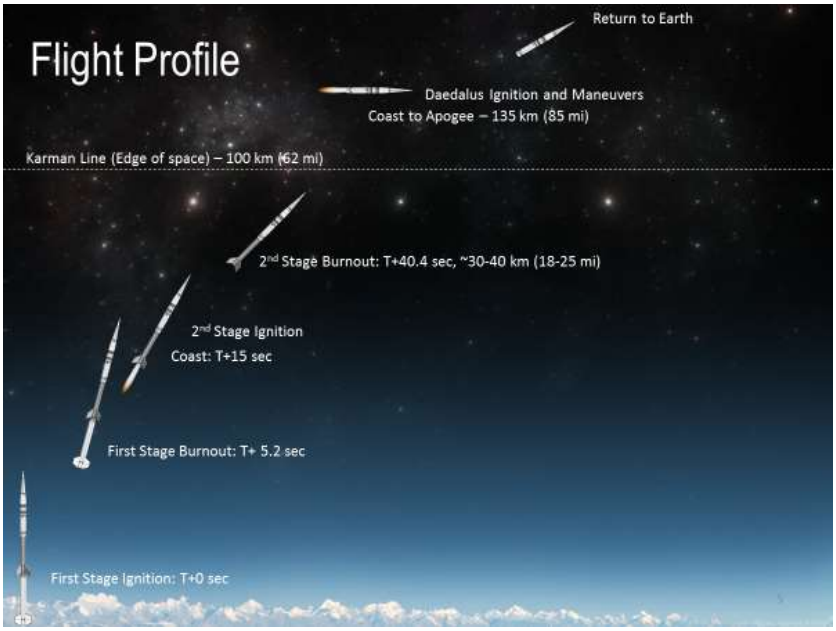

Figure 3 DEADALUS Flight Profile

To demonstrate the main and reaction control engine capabilities, the vehicle will perform various maneuvers and finally the RCEs will orient the vehicle reentry position to come back.

2.2 Research Opportunities

Many rocket engines use a film of liquid as cooling method for protection for the combustion chamber walls. The current CROME engine design will use fuel film cooling (FFC); this method works by generating a film of fuel into the chamber that will serve as a thermal barrier

between the combustion gases and the combustion chamber. This method was selected due to its simplicity, but future versions will attempt to implement a regenerative cooling design.

Additive manufacturing is a growing technology which process consists of digital 3D design data to build up components in layers by depositing material. The benefits from this technology lie in those areas where conventional manufacturing reaches its limitations. It provides a high degree of design freedom, optimization and integration of functional features. Future versions of CROME will try to successfully incorporate components made by using additive manufacturing.

CHAPTER 3: Liquid-Propellant Rocket Engines

The main function of a rocket engine is to generate thrust through combustion. The force generated transmits a momentum to the combustion products and a momentum in the opposite direction. The thrust generated by a rocket is the reaction experienced by the structure when ejecting high velocity gases. Thrust can be divided into two terms, momentum and pressure thrust. Momentum thrust is the product of the propellant mass flow rate and the exhaust velocity relative to the vehicle and it accounts for the majority of the thrust generated by a rocket. Pressure thrust is the product of the cross sectional area of the exhaust jet leaving the vehicle and the difference between the exhaust pressure and the surrounding fluid pressure (ambient pressure) (Huzel & Huang, 1992).

The operation of a rocket engine system is independent of its environment except for effects on performance cause by ambient air pressure. A conventional engine configuration is shown in Figure 4. A converging nozzle accelerates the gases until it reaches the throat; because of compressible flow effects, the gas reaches sonic velocity or Mach 1. When the gases reach this velocity, increasing the flow area further increases the velocity of the gases. Because of this, to reach sonic velocity, a diverging nozzle must be used. Figure 4 shows a chamber and nozzle configuration:

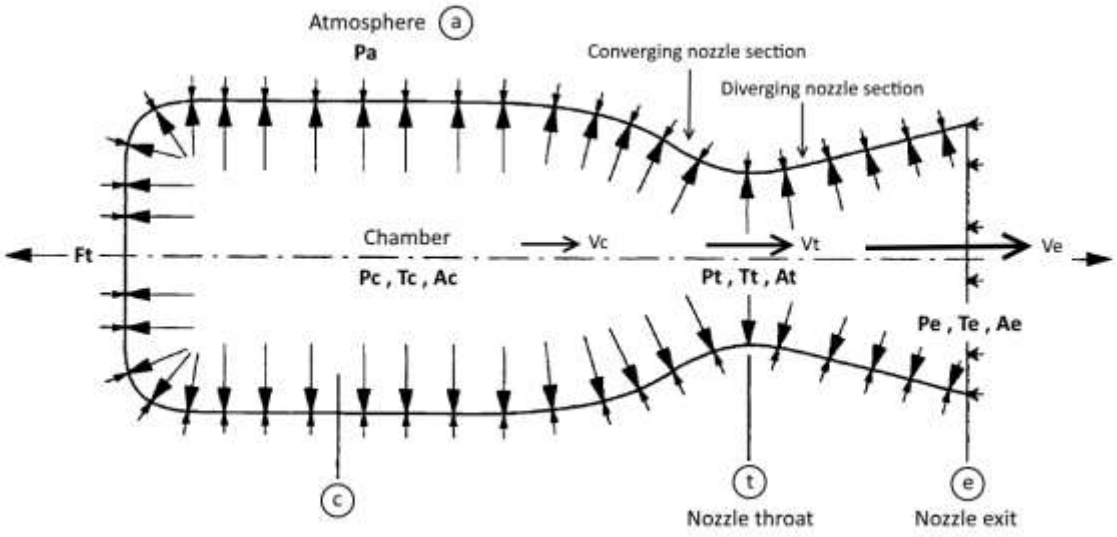

Figure 4 Rocket Engine Chamber and Nozzle Configuration

3.1 Pintle Injector

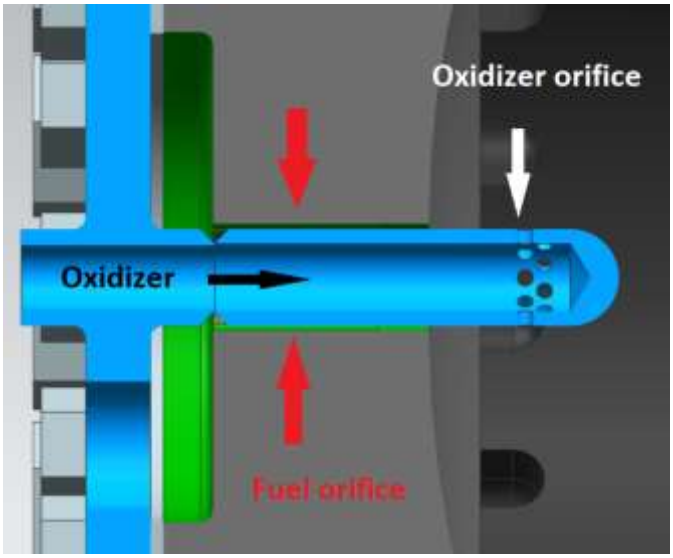

Figure 5 Pintle Injector Design

CROME will use a pintle injector as the injection method. The pintle injector rocket engine is fundamentally different from other rocket engines, which nearly universally employ a series of separate propellant injection orifices distributed across the diameter of the headend of the combustion chamber. The pintle's central, singular injection geometry results in a combustion chamber flow field that varies greatly from that of conventional rocket engines. These differences result in certain operational characteristics of great benefit to rocket engine design,

performance, stability, and test flexibility (Atyam & Hguyen, 2015). The basic concept of the bipropellant pintle injector is shown in Figure 5.

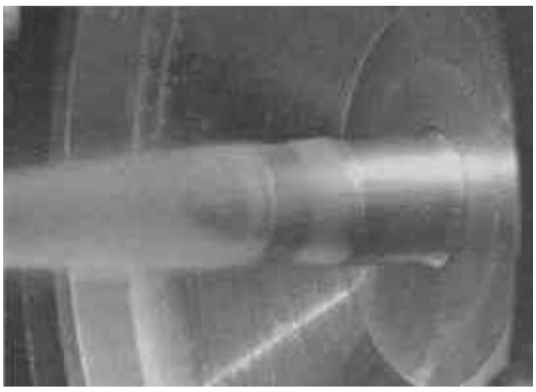

Figure 6 Inner Flow Only (Dressler & Bauer, 2000)

Figure 7 Outer Flow Only (Dressler & Bauer, 2000)

Figure 8 Combined Flows (Dressler & Bauer, 2000)

The 90°, axial-radial impingement of the two propellant streams combined with the specific geometry of the resulting atomization and mixing "fan" is fundamental to the pintle injector providing both high combustion efficiency and inherent combustion stability. The impingement point is within the chamber distance down the axis of the post from the injector face, also known as the skip distance. Figure 6, 7, and 8 show a representation of the annular injection, radial injection, and the spray fan resulting from the combined injected flows (Dressler & Bauer, 2000).

Pintle injectors are well known for their deep throttling capabilities, low cost compared to impinging type injectors, and high combustion efficiency. Pintle injectors typically deliver high combustion efficiency in the range of 96-99% (Dressler & Bauer, 2000). Deep throttling is done using an actuation mechanism that displaces the sleeve of the pintle post axially.

Chapter 4: CROME Design Requirements

The mission's top level requirements became design drivers for this engine. As the design process evolved, many iterations were conducted to fulfill mission requirements. Top level requirements will be discussed on this chapter.

4.1 Torch Igniter Requirements

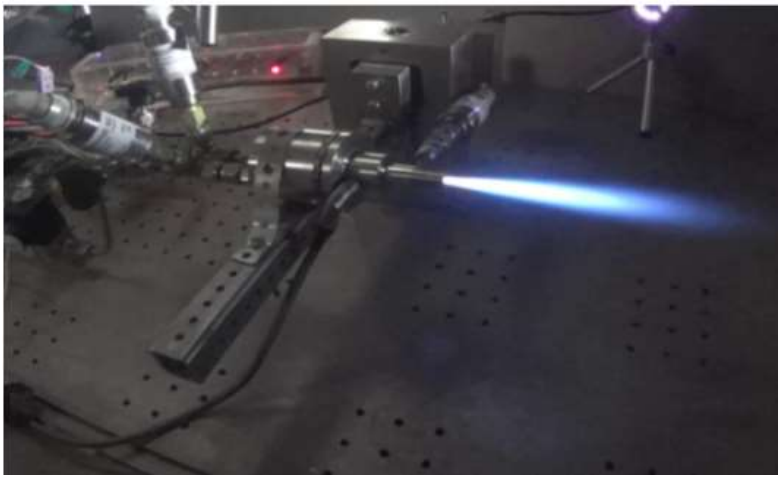

Figure 9 Torch Igniter Testing

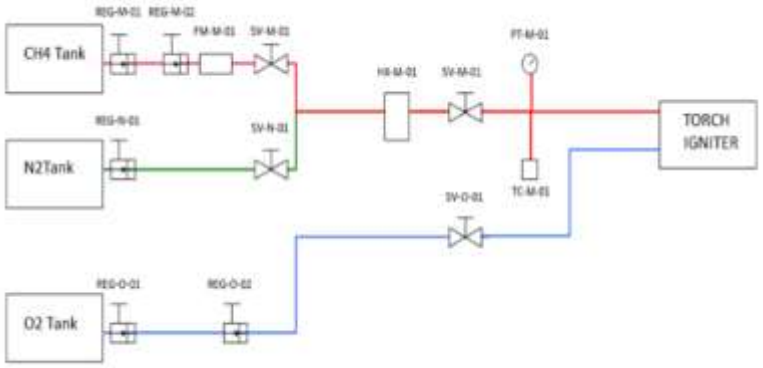

Figure 10 Torch Igniter Schematic

The torch ignition system was designed as the source of ignition for CROME. A swirl coaxial igniter was fabricated after a series of experiments to characterize methane's properties and performance as a rocket fuel. This type of igniter introduces oxygen through an axial orifice while the methane is injected in a tangential swirl pattern around the combustion chamber. The main requirement of the igniter is that is should ignite the propellants at gaseous state.

Several iterations of the sparking system were manufactured in-house until it was decided to use an already manufactured spark plug. This spark plug was smaller than the previous ones

used allowing to place it closer to the methane injection ports. 100% ignition rate was achieved with this method with the use of gaseous propellants. Two solenoid valves will be used to control the flow going into the igniter. Additional instrumentation will be used to verify the pressure and supplementary support will be used to attach the apparatus to the engine envelope.

4.2 Operational Requirements

The requirements discussed previously are shown in Table 1 and Table 2. Various calculations were done using CEA (Chemical Equilibrium with Applications) and RPA (Rocket Propulsion Analysis) software to accurately determine the thermodynamics properties of different propellants to perform rocket engine analysis.

Table 1 DEADALUS Requirements

Requirement	Definition / Value
Thrust, (Ft)	125 – 500 lbf (4:1 throttleability)
Operation Pressure	12.8 psia (ambient), and 0 psia (space)
Propellants	LOX/LCH4 (Liquid Oxygen/Liquid Methane)
Propellant Tank Pressure	400 psia
Cooling Method	Film Cooling
Reaction Control Engines	12

Table 2 Derived Engine Requirements

Requirement	Definition / Value
Chamber Pressure (Pc)	70 – 235 psi
Specific Impulse (Isp)	227s (sea level), 330s (vacuum w/o cooling)
Injector Type	Pintle Injector

Nozzle Shape & Expansion Ratio (ϵ)	Bell Shape ϵ: 1.6 for sea level testing, 30 for space operation
Mixture Ratio	Combustion: 2.7
Type	Steady State Engine
Material	Inconel 625 (Injector Components) Inconel 715 (Thrust Chamber)
Cooling Method	≤ 30% fuel film cooling
Envelope	≤ 14.5 Diameter ; ≤ 24 " Length

4.2.1 Mixture Ratio

To find the optimal mixture ratio (MR), a chart was generated using CEA and RPA using a chamber pressure of 235 psi and our two propellants (LOX & LCH4) plotting the MR against specific impulse (Isp). After analyzing the chart, we can see that that optimal mixture ratio is around 2.7. The reason behind this is because this number allow us to have equal tank sizes. This happens because the density of liquid oxygen is roughly 2.7 greater than the density of liquid methane, leading to equal propellant volume. Having equal tank sizes simplifies engine design.

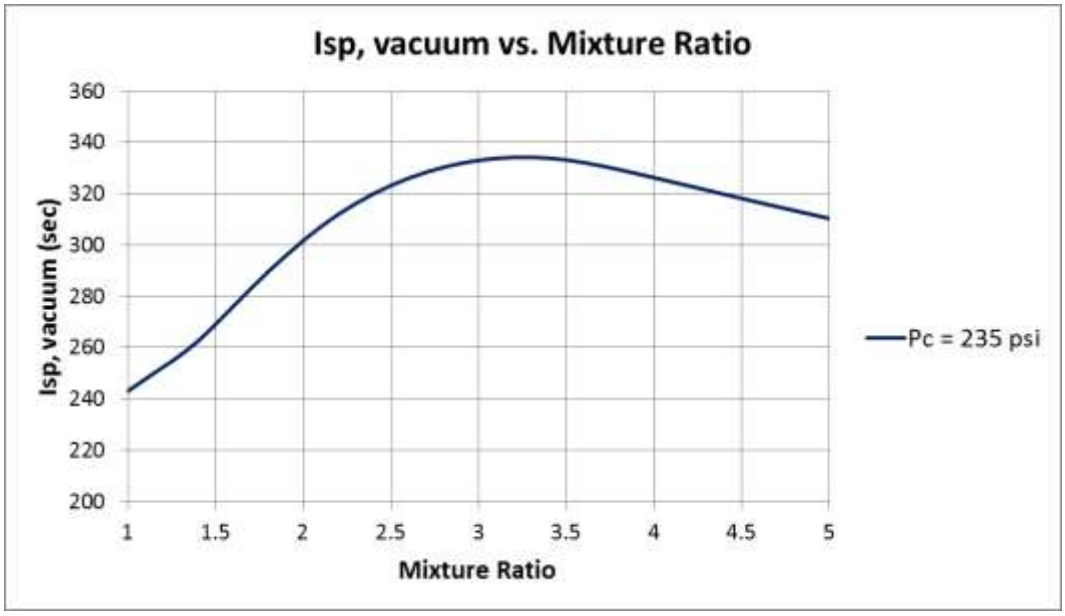

Figure 11 Specific Impulse (Isp) vs. Mixture Ratio (MR) for LOX/LCH4 Propellants

4.2.2 Material

Each component of the engine will be exposed to different loading conditions. The engine will experience cryogenic temperatures from the propellants and hot temperatures due to combustion. Because of this, the materials selected to manufacture this engine were Inconel 718 and Inconel 625. This material is ideal for aerospace applications because is compatible with LOX and LCH4 and can withstand hot and cryogenic temperatures. Inconel 718 has a relatively high melting temperature of 2300-2437 °F, however, the maximum temperature allowed will be 2000 °F during operation. Inconel 625 offers similar mechanical properties as Inconel 718, nonetheless, Inconel 718 is stronger (180 vs 120 ksi ultimate strength at room temperature). Because of this, the chamber will be made out of Inconel 718 due to the high temperature this part will be exposed. Stainless Steel 316 will be used for the propellant lines going into the injector because it is the easiest to find and a less expensive option to other alloys.

4.2.3 Fuel Film Cooling

During combustion, chamber walls can reach temperatures over 4500 °F, these temperatures are able to melt any material by a large margin. As a result of this, a cooling method is required. The method chosen was fuel film cooling (FFC) in which a percentage of the fuel (30%) used for combustion is injected along the surface of the wall that acts as a thermal barrier between the chamber wall and the combustion gases. This percentage was the same that NASA Johnson Space Center Morpheus project used for their Morpheus LOX/LCH4 engine.

4.2.4 Nozzle Shape & Expansion Ratio

To reach supersonic velocity, the ratio between the exit pressure and chamber pressure has to be lower than the critical pressure ratio. This pressure is defined in Equation 3:

$$\frac{P_t}{P_c} = \left(\frac{2}{k+1}\right)^{\frac{k}{k-1}} \qquad \textit{Equation 1}$$

Where:

P_t: pressure at the throat

P_c: chamber pressure at the nozzle

k: specific heat ratio of the gas

If the pressure ratio between P_e and P_c is greater than the critical pressure ratio, the flow will not reach sonic conditions and the divergent nozzle will slow down the gas instead of increase the velocity (Sutton & Biblarz, 2010). To achieve maximum performance in El Paso, TX the expansion ratio has to deliver ideal expansion (P_e=P_a). Because the engine will throttle, is preferable to use an under-expanded nozzle.

A space operation expansion ratio was selected due to weight constraint and dimensions set by the vehicle and driven by the thrust and performance increase. The following picture shows the analysis done to help select the expansion ratio comparing it with Isp, thrust, and weight:

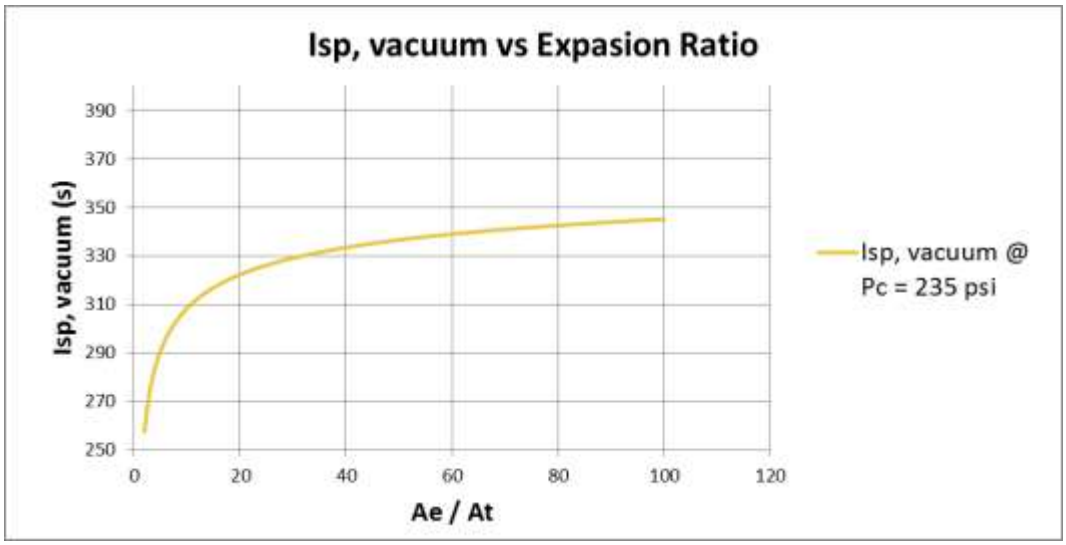

Figure 12 Isp vs. Expansion Ratio @ 235 psia Chamber Pressure

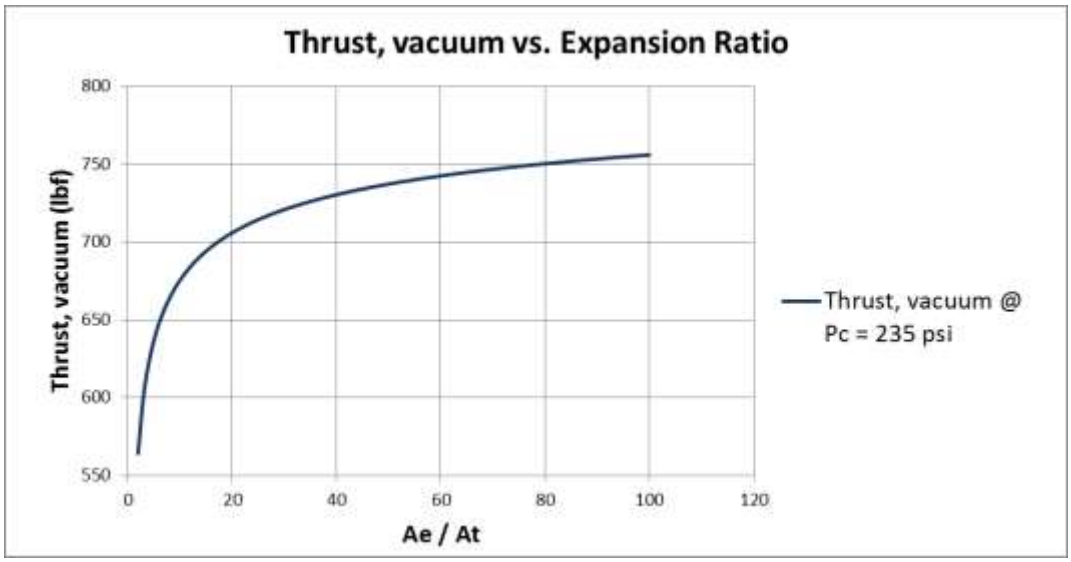

Figure 13 Thrust vs Expansion Ratio at 235 psi Chamber Pressure

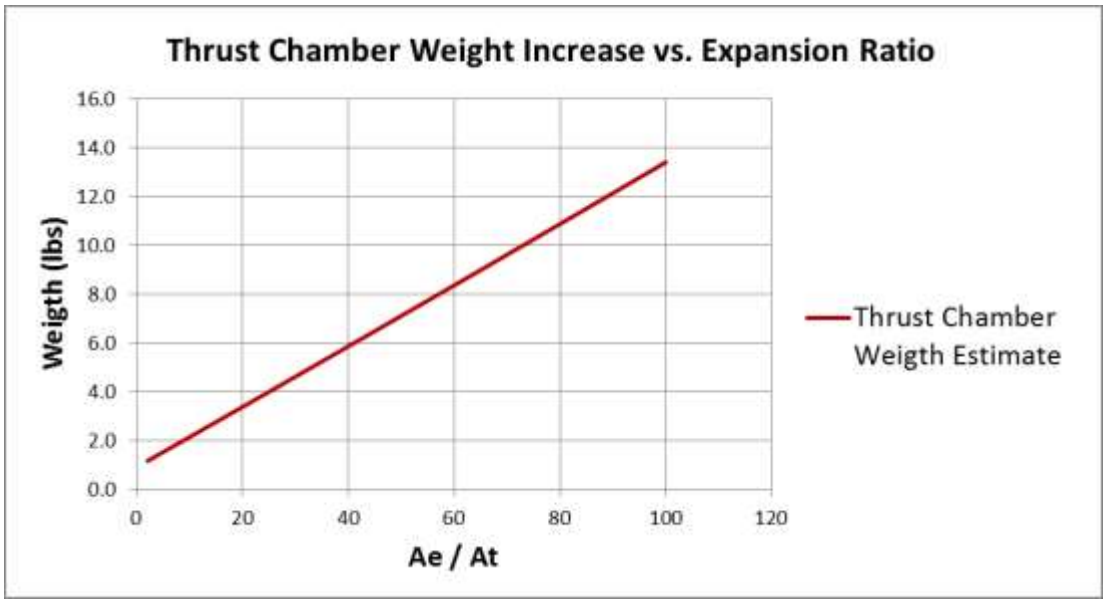

Figure 14 Thrust Chamber Wight Increase Estimate vs Expansion Ratio

Thrust and Isp start to asymptote at approximately 60, but because of weight constraint, an area of expansion of 30 was chosen for space operation.

4.2.5 Envelope

The size and weight of the engine is defined by the mission. The engine consists of five components, thrust chamber, injector body, manifold cap, pintle post, and acoustic cavities. The whole package, including the valves and any plumbing and fittings has to fit inside an envelope of 14.5” in diameter and 27” in length and weight no more than 70 lbs. The size of each component will be described further on this thesis. Figure 15 shows a cross-section of the whole assembly and Figure 16 show the size envelope:

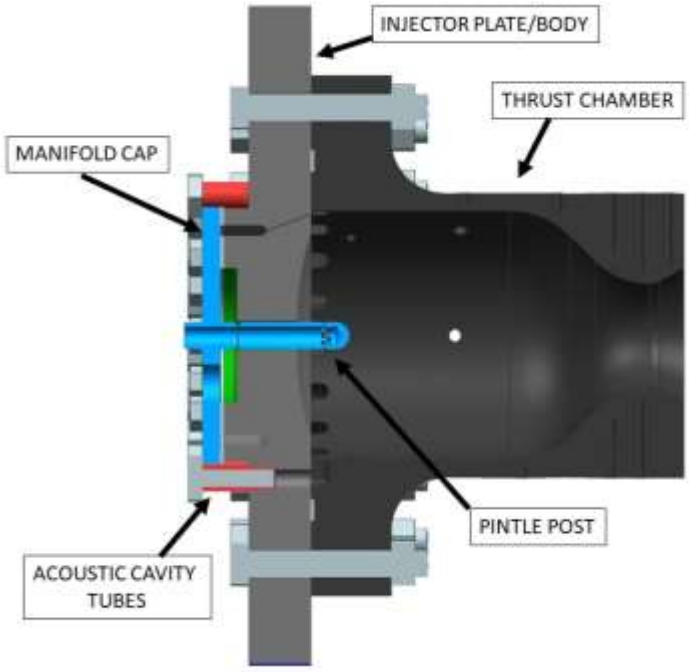

Figure 15 CROME Components

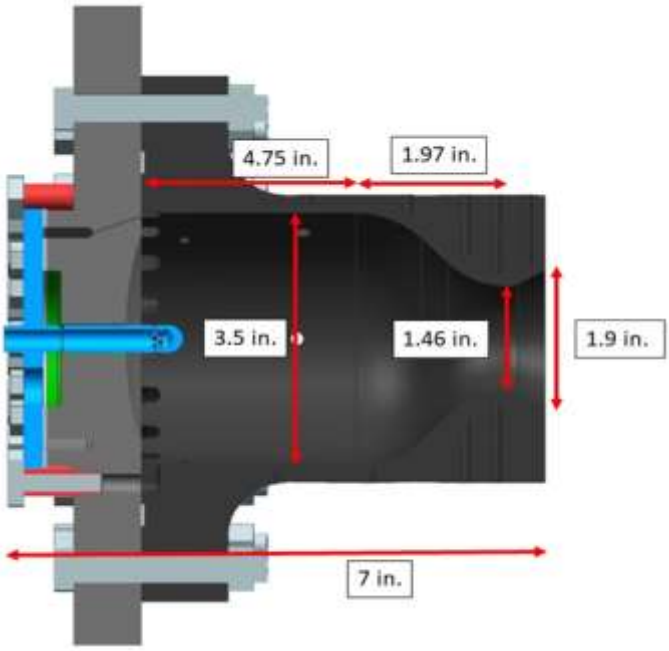

Figure 16 CROME Size Envelope

4.2.6 Chamber Pressure (Pc)

Chamber pressure was chosen according to the throttling requirement. The requirement states the engine should have the capability to throttle to a ratio 4:1, that is, 125 lbf to 500 lbf. The required pressure to have sonic flow at the throat is 35 psi at sea level. Because of this, it was determined to choose 70 psi to be the low end thrust and 235 the maximum operating pressure.

4.2.7 Propellant Feed System

The propellant feed system is a key component for rocket engine design, it delivers the propellants from the tanks to the thrust chamber. A pressure-fed design was chosen because we are relying on the tanks to feed the propellants into the thrust chamber. In general, pressure-fed engines have a more simple design because we do not need the use of turbopumps which will add weight and are unreliable under space conditions.

The propellants would fill the lines as well as the propellant which would be left unused in the tank after the flight is done. The tanks that will be used were sized according to the requirements of the main engine. Preliminary design of these tanks was made based on the design made by Morpheus. Johnson Space Center provided computed assisted drawings (CAD) and various modifications were made to them in order to fulfill DEADALUS requirements.

Another important subject are the tanks that will be used for flight. For flight, tanks were designed by the cSETR, they must allow storage of the two propellants and the pressurization gas separately. They are used to pressurize the propellants and ensure that the engine will receive the necessary fuel to burn and deliver thrust. They also must carry enough propellant to ensure that main mission objectives and ancillary maneuvers can be achieved successfully. One of the most important constraints for tank sizing was the DEADALUS size envelope. However, for the first

stages of testing, it was recommended to use 6K type cylinder by Air Liquide, one of the suppliers at the tRIAc facility. Although it is more than the required amount, extra GN_2 can be delivered for purging purposes during testing.

Chapter 5: Combustion Instabilities

One of the most critical and most dangerous phenomena occurred in a rocket engine are combustion instabilities. This is because if not treated with some form of dampening, they can lead to engine failure due to destructive vibration. These vibrations can damage the chamber and/or decrease engine efficiency. The design of the acoustic cavities for CROME used to lower the impact of this behavior are discussed in detail in the thesis written by Jonathan Candelaria.

Combustion Instabilities have been recognized and studied since the beginning of rocket engines in the 1930s. Combustion instabilities are oscillations produced largely by pressure. We can see this behavior in almost all rocket engine programs and still there is no exact way to avoid them. The best way to tackle this problem is by identifying the main type of instabilities which are low (10-400 Hz), medium (400-1000 Hz), and high (<1000 Hz) frequency instabilities.

These frequencies can also see different modes that include the axial component, longitudinal mode, and transverse component, tangential and radial modes, or a combination of these. Figure 17 shows a visual representation of these modes.

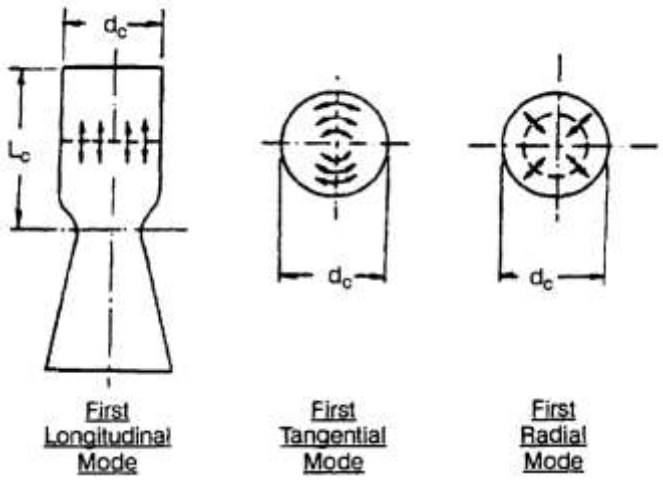

Figure 17 High-Frequency Modes

These frequencies cause acoustic modes that equal that of cylindrical volume. Analysis was done to estimate the corresponding resonant frequencies at which each mode will occur using the following formula:

$$f_{m,n,q} = \frac{c}{2\pi}\sqrt{\left(\frac{\lambda_{mn}}{R_c}\right)^2 + \left(\frac{q\pi}{L_c}\right)^2}\ ,\ (Hz) \qquad \textit{Equation 2}$$

Where:

c: speed of sound

λ: transversal eigenvalues for tangential and radial mode

m,n: 0,1,2…

q: longitudinal mode number

R_c: combustion chamber diameter

L_c: effective acoustic length

The acoustic frequencies for CROME are shown in Table 3:

Table 3 Calculated Acoustic Modes for CROME

Acoustic Modes	Resonant Frequency (Hz)
1L	5095.6
2L	10191.3
3L	15286.9
1T	6416.5
1T1L	8193.7
2T	10643.8
2T1L	11800.7
1R	13353.4
1R1L	14292.6
2R	24449.2
2R1L	24974.5
3T	14641.1

Through the calculations and models performed in MatLab we were able to identify the three acoustic modes and its resonant frequencies which would have a greater impact to the engine. These frequencies are the three highlighted rows in the Table 3. Now that we have identified them, these will be the frequencies we will try to dissipate.

5.1 Acoustic Dampening Mechanisms

Pressure fluctuations in the combustion chamber can reduce the efficiency of the system or, in the worst case scenario, these fluctuations can resonate with the engine acoustics then excessive vibration forces will lead to engine failure. There are different ways to dissipate these frequencies to stabilize the system. The method selected for our engine are called acoustic cavities. These cavities try to maximize the acoustic absorption of the frequencies mentioned before. These cavities will be lined across the combustion chamber near the injector. The dimensions of the cavities were sized according to the predicted frequency at which the instability manifests. Figure 18 shows the acoustic configuration for CROME:

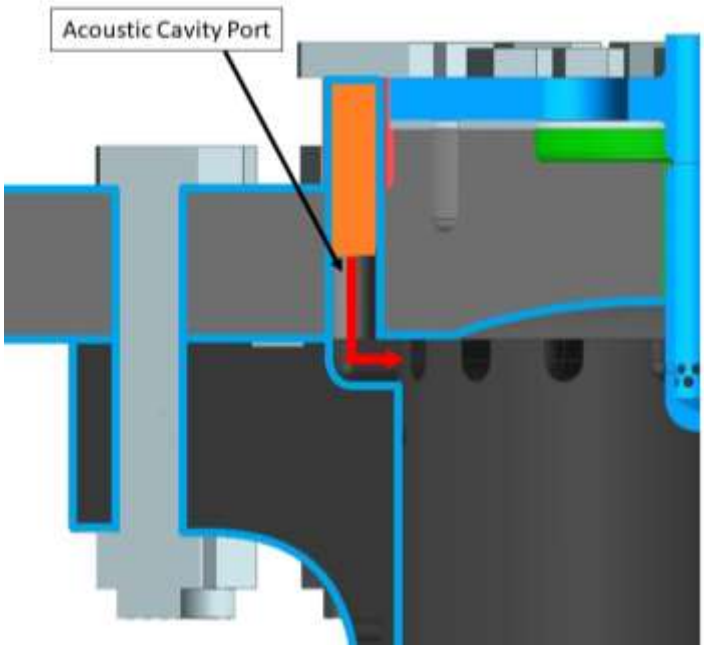

Figure 18 Acoustic Absorber Configuration

17 equally spaced cavity ports will be used for CROME. These resonators were chosen because they were easy to integrate to our system and can be “tunable” by adding a screw to vary the length by changing the cavity volume.

Chapter 6: CROME Design Analysis

To have a more accurate analysis of the system, each major component was studied separately. The analysis was performed this way, because each component will experience different loading conditions. Finite Element Analysis (FEA) was done to verify structural and thermal integrity of the engine. In order to complete FEA, the requirements for each component were defined and a safety factor of 1.5 was implemented based on the yield strength of the material. After the analysis, the components should not experience stresses which exceed the yield strength of the material and must maintain the 1.5 safety factor. Each model concept was developed with Altair Hypermesh. The objective was to find areas of high stress and then modify the design if necessary.

6.1 Thrust Chamber

The thrust chamber may be the most recognizable part of a rocket engine. Almost all rocket engines use a cylindrical design because they provide less cooling requirements and encounter less mechanical stress due to smaller surface area. This is where the propellants mix and combustion takes place. The chamber must follow a converging-diverging profile with a bell nozzle that can produce 500 lbf of thrust. The design must have provision for thermocouples that will be placed along the axial and radial directions of the thrust chamber focusing attention on the throat, where the heat flux is at its highest. Also, it must have provisions for static and dynamic pressure transducers to measure the pressure inside the chamber. Upon testing the thrust chamber will choke fluid flow at the throat ($A_t < A^*$). If this does not occur then it will be considered a failure. The interface to the injector will be provided for interchangeability of components. Combustion chamber must be functional for a pressure range of 0 to 235 psi where 235 psi is the maximum operating pressure and a maximum allowable pressure of 700 psi. A factor of safety of 1.5 to yield

must be met for the maximum allowable pressure induced stresses. Due to the high and cryogenic temperatures, the material used for the chamber will be Inconel 718 and must withstand the stresses induced by chamber pressures and thermal stresses. From a melting standpoint, it must not be heated to or above its melting point during combustion of propellants.

To find the nozzle profile, the thermodynamic properties of our propellants were found using NASA Chemical Equilibrium with Application (CEA) software. This was necessary in order to find the diameter of the thrust using the following equation:

$$C_f = \sqrt{\frac{2\,k^2}{k-1}\left(\frac{2}{k+1}\right)^{\frac{k+1}{k-1}}\left[1-\left(\frac{P_e}{P_c}\right)^{\frac{k-1}{k}}\right]} + \left(\frac{P_e - P_a}{P_c}\right)\epsilon = 1.3 \qquad \textit{Equation 3}$$

Where:

C_f: Thrust coefficient, the increase of thrust provided by the gas expansion through the nozzle

k: specific heat ratio

P_c: chamber pressure

P_a: atmospheric pressure

P_e: pressure at the exit

The next step was to find the diameter of the throat using the following equation:

$$A_t = \frac{F_t}{P_c\,C_f} = \frac{500\ lbf}{235\ psi * 1.3} = 1.68\ in^2 \qquad \textit{Equation 4}$$

This yield a diameter of 1.46 in.

Lastly, the characteristic length or L* (the ratio between the volume of the chamber and the area of the throat was found using the following equation:

$$L^* = \frac{V_c}{A_t} \rightarrow V_c = 36\ in^3 \qquad \textit{Equation 5}$$

Using these values, the first design of the thrust chamber was designed. Figure 19 shows the first design of the thrust chamber. The profile of the nozzle was taken from RPA by determining the thermodynamic properties of our propellants, chamber pressure, and desired thrust. The idea was to attach the thrust chamber to the structure using 4 bolts and weld the corresponding thermocouples along the surface of the nozzle. However, this configuration would create major stress on the attachments and the manufacturing cost would increase significantly due to the complicity of manufacturing a nozzle. Lastly, preliminary analysis showed that the wall thickness would not pass the FoS requirement.

Figure 19 Thrust Chamber First Iteration

The next thrust chamber design was selected due to it being more accessible in the manufacturing process. Also, since the first tests will be ground based, the weight itself will not be a major factor as it would be on actual flight tests. The geometry of the thrust chamber can be seen in Figure 20, Thermocouple ports are also visible along the surface of the nozzle profile. Another major change from the first iterations of the design, was the igniter placement, from the top to the surface of the

chamber. This will allow more space on top of the engine for the main valves and feed system. Provisional support will be provided for the igniter assembly.

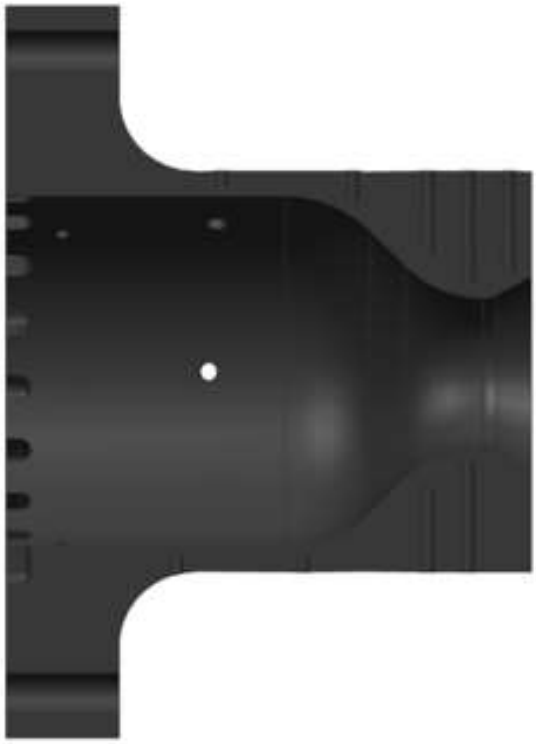

Figure 20 Last Iteration of Thrust Chamber Geometry

Wall thickness was increased from 0.1 in to 0.25 in after performing a thickness analysis to find the optimal thickness that would satisfy thrust chamber structural requirements. For this, we found the vonMisses stress using Equation 5:

$$\sigma_v = \sqrt{\sigma_h^2 + \sigma_l^2 + (\sigma_h * \sigma_{l)}} \qquad \textit{Equation 6}$$

Where:

σ_h: Hoop stress

σ_l: Longitudinal stress

To find the Hoop and Longitudinal stress we use the maximum expected P_c and inner diameter of the chamber. Dividing 11750 psi (Inconel 718 yield strength @ 2000 °F) over the vonMisses stress

of 6813 psi, we have a FoS of 1.72, meeting thrust chamber structural requirements (see Appendix).

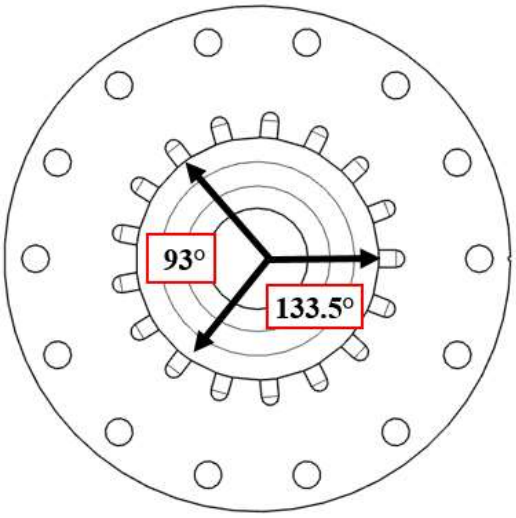

Figure 21 Dynamic Pressure Transducers Configuration

The placement of the dynamic pressure transducers should be such that they should not be damaged during hot fire testing. Figure 21 shows the placement of the dynamic pressure transducers that will be used to validate frequencies.

In order to begin the study of this component, we found the bolt preloads on the thrust chamber flange. A required 2500 psi is needed for the GORE seal to seal according to the manufacturer. To find the total force needed to seal we use Equation 6:

$$F_c = \left(A_c * P_g\right) + \left(P_c * A_{cc}\right) \qquad \textit{Equation 7}$$

Where:

A_c: compressed contact area

P_g: required GORE seal pressure

P_c: chamber pressure

A_{cc}: chamber contact

A total preload of 2443 lbf per bolt is required to seal using 14 UNC (3/8)-16 bolts (see Appendix).

We can take advantage of the chamber's geometry using quarter symmetry to reduce the domain by a factor of 4. The reduction in analysis domain could mean a finer mesh that can be used in the reduced analysis domain yielding more accurate results. The reduction in

computational time also plays an important role in the analysis. A mesh was created using Hypermesh 3D elements with a minimum element size of 0.05 in.

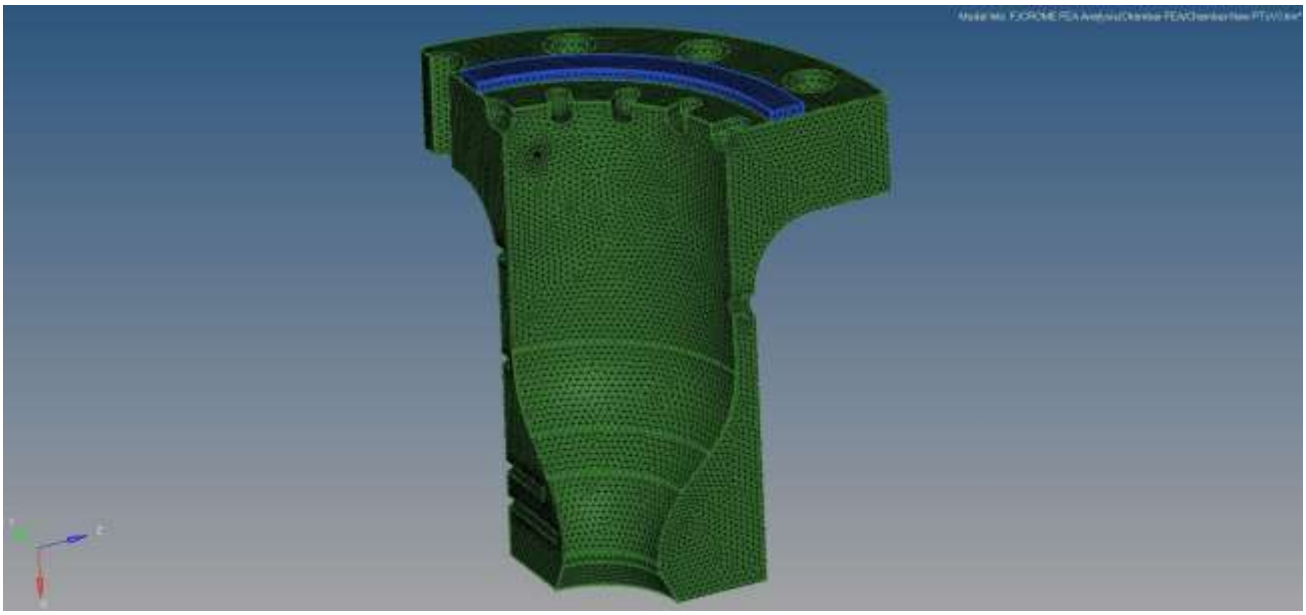

Figure 22 Combustion Chamber Mesh

The following table shows the loads applied to the thrust chamber:

Table 4 Combustion Chamber Loading Conditions

Figure	Load	Value
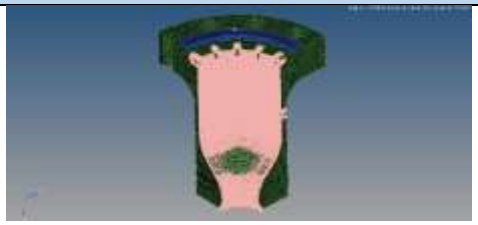	Temperature SPC	1700 °F
	Quarter-Symmetry SPC	N/A

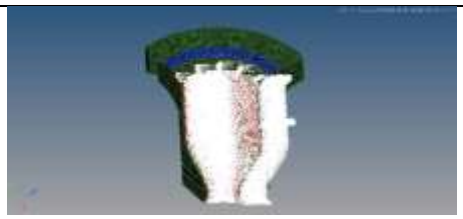	Chamber Pressure	700 psi
	Chamber Bolt Preload Pressure	2440 lbf

The FEA on the chamber was performed after the first iteration of the design was done. We can observe on Figure 23 that the area that has the largest stress levels, close to 30000 psi, is the thin part of the main chamber body. Also, the acoustic cavity holes experience higher stress levels similar to those in the main body. However, the experienced stresses by the chamber will not compromise the design since these stress levels are lower than that of Inconel 718 yield strength of 150000 psi at 1700 °F. This stress phenomena was seen since the first iterations of the analysis on the chamber design. To reduce the stresses, we opted to thicken the chamber flange from 0.25 in to 1.125 in.

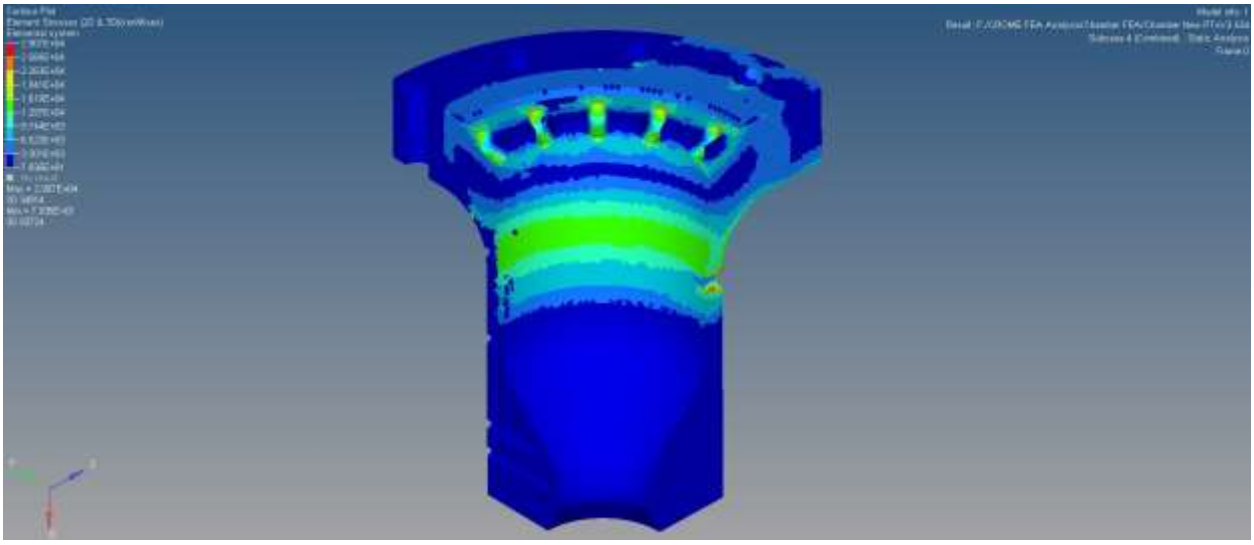

Figure 23 Chamber Stress Contours

6.2 Injector Body

This part of the engine puts the propellants in the combustion chamber, it atomizes, distributes, and mix the propellants into the appropriate ratio of fuel and oxidizer. The design determines the maximum achievable combustion efficiency, the heat transfer rated to the combustion chamber walls, and whether or not low and high frequency combustion instabilities will occur (Yang, Habiballah, Hulka, & Popp, 2004). No other component of a rocket engine has greater impact upon engine performance, each percentage point loss in injector combustion efficiency (c*) means a loss of the same magnitude in overall specific impulse (Isp) (Douglass, Combs, & Keller, 1975). The first design of the injector body can be seen in Figure 24. This design has an igniter port before we decided to place the igniter on the chamber.

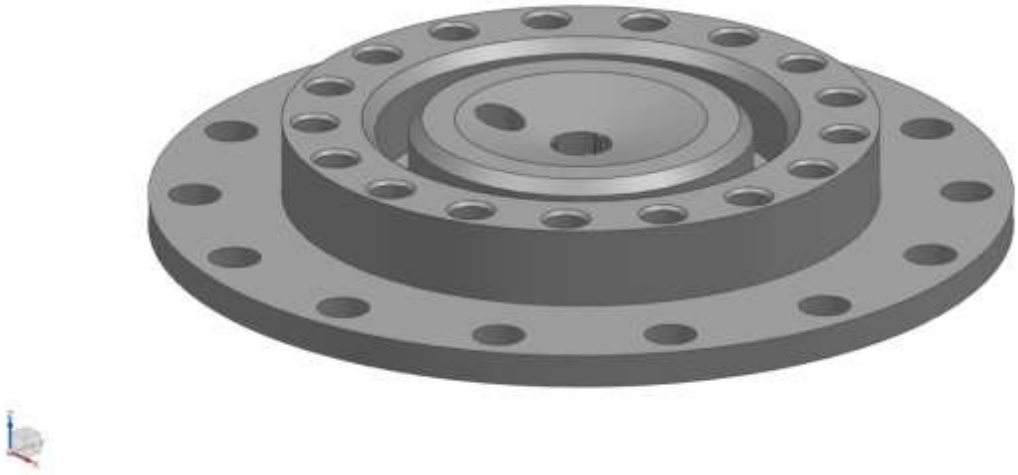

Figure 24 Injector Body First Iteration

During the 2017 Southwest Emerging Technology Symposium, Mark Klem, chief of the Chemical Propulsion Systems Branch at NASA Glenn Research Center, reviewed our design and

recommended to switch out design from fuel centered to LOX centered, meaning the liquid oxygen would go through the pintle, and liquid methane through the injector body orifice. The main concern from the first design was the GORE seal reliability. Figure 25 shows a cross-section of the fuel centered design:

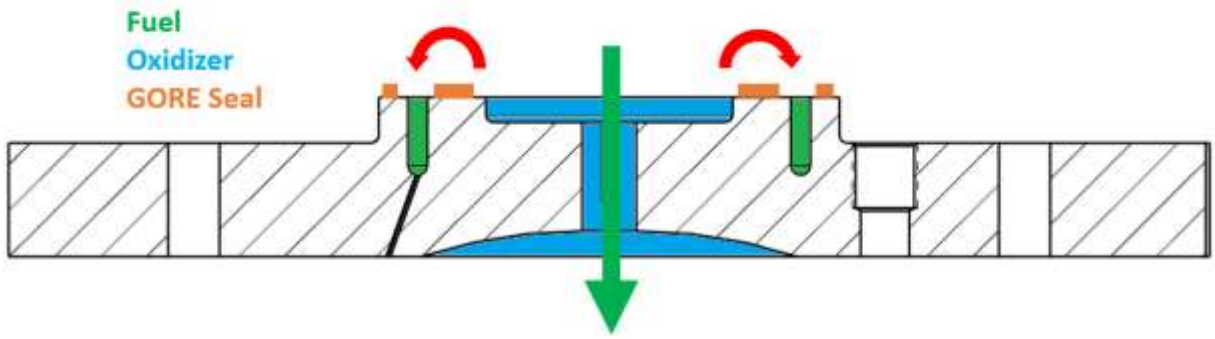

Figure 25 Injector Body Fuel Centered Design

In a worst-case scenario of having back-flow from the ignited fuel to the manifold, the whole engine would fail. The new injector body geometry is displayed in Figure 26:

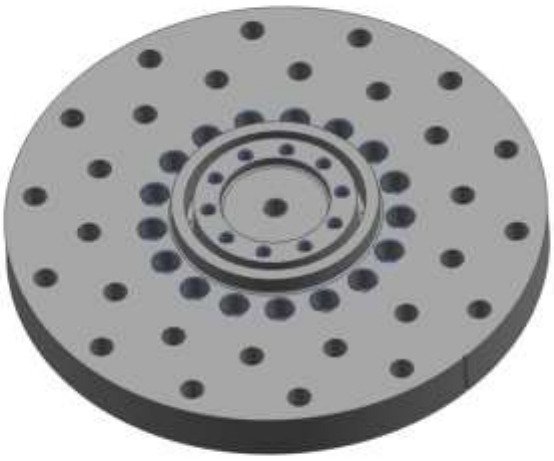

Figure 26 Injector Body Geometry

A non-permanent sealed interface will be used for the first stage of testing for mounting of injector to pintle manifold and thrust chamber meeting gasket requirements. This allows for interchangeability of components for conditions such as failure, varied condition firing, etc. GORE seal will be used to maintain the propellant within the thrust chamber and the injector body. The seal must prevent leaking of propellant into the atmosphere. A film cooling channel must be provided to avoid melting temperatures. 30% of the fuel flow rate for combustion is going to be used for cooling (0.5-0.18 lbm/s). The material selected for the injector was Inconel 625 due to its strength properties discussed before and weldability to other like components. Conventional machining operating will be used to manufacture the injector body.

The injector must be functional for a pressure range of 70-235 psi where 235 psi is the maximum operating pressure. A factor of safety of 1.5 to yielding must be met for pressure induced stresses. No structural failure should occur i.e. plastic deformation, melting, or pressure stress cracks. The pressure ranges from 75 to 235 psi at full thrust, however, a pressure spike of 700 psi is expected.

A bolted configuration will be used to interface the injector body to thrust chamber, a second configuration to interface injector body to the structure, and a third configuration to the manifold. The interface from injector body to thrust chamber should be such that the injection of propellants into the combustion chamber is reliable. The bolts used must not pass 90% proof load and must apply the sufficient pressure to the GORE in order to have a reliable seal. 14 (3/8)-16 bolts will be used to connect the injector body to the thrust chamber. The bolt analysis was described in section 6.1.

The following boundary conditions for the simulation have been applied. On Figure 27 we can see the injector body geometry from a top view. In green and orange a bolt preload to be

applied on top on the outer and inner circle of bolts respectively. As on the middle circular structure. The top faces of these circles will have a GORE seal Pressure represented in red.

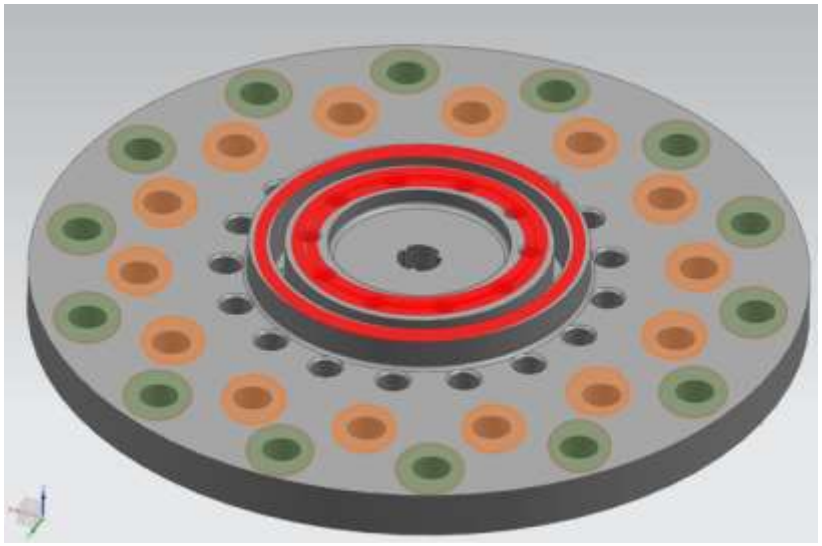

Figure 27 Bolt Preload and GORE Seal Load Conditions Top Distribution

In Figure 28 we can see the body of the injector but now from a bottom view. The blue outer circle will be the fix underside of the bolt area. The orange inner circles represent the bolt preload on the bottom and the red circle represents the applied GORE seal pressure from the bottom view.

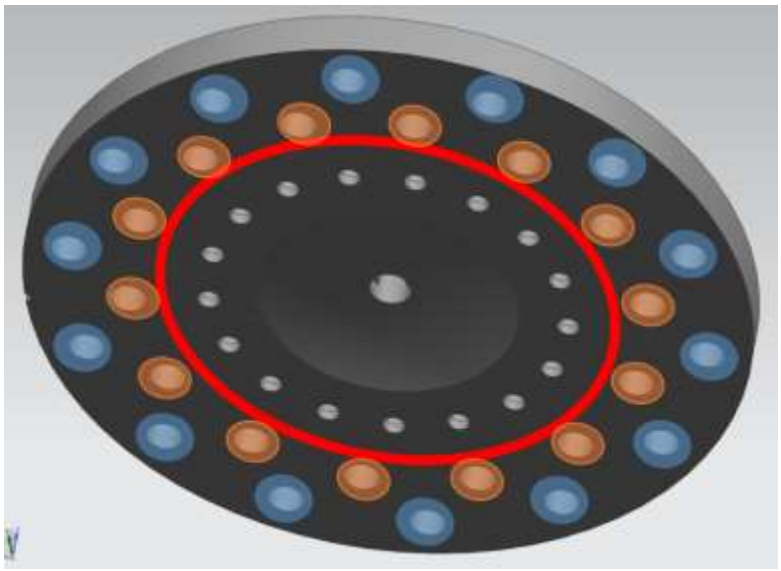

Figure 28 Bolt Preload and GORE Seal Load Conditions Bottom Distribution

Just like with the chamber geometry, the injector's geometry can be used with quarter symmetry to reduce the domain by a factor of 4. The domain reduction means a finer mesh which will yield more accurate results. The reduction in computational time also plays an important role in the analysis. A mesh was created using Hypermesh 3D elements with a minimum element size of 0.01 in.

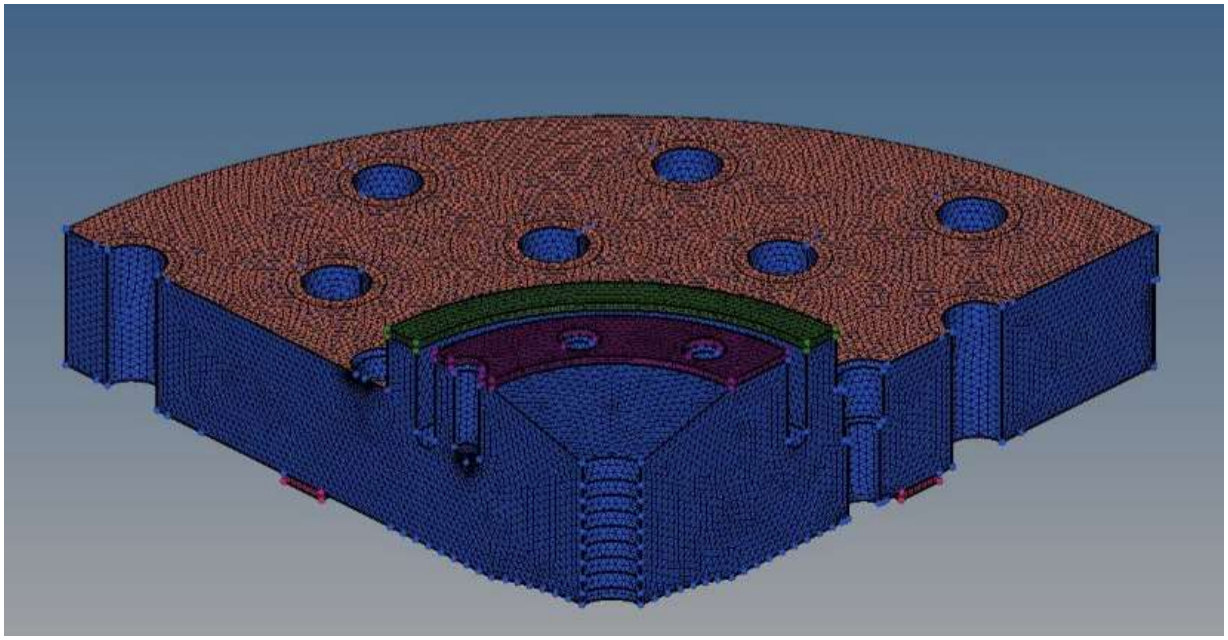

Figure 29 Injector Body Mesh

A finer mesh was generated around the end of the acoustic cavity holes and bolted connection to thrust chamber. This was done because, in the first iterations of the analysis, .the cavity holes and bolted connection to thrust chamber, were the areas where we found higher stress. After analyzing the stress areas, modifications to the design were made to sustain the stress to acceptable levels where it would not compromise the design. To reduce the stress on these areas, we opted to thicken the injector thickness from 0.5 in to 0.875 in.

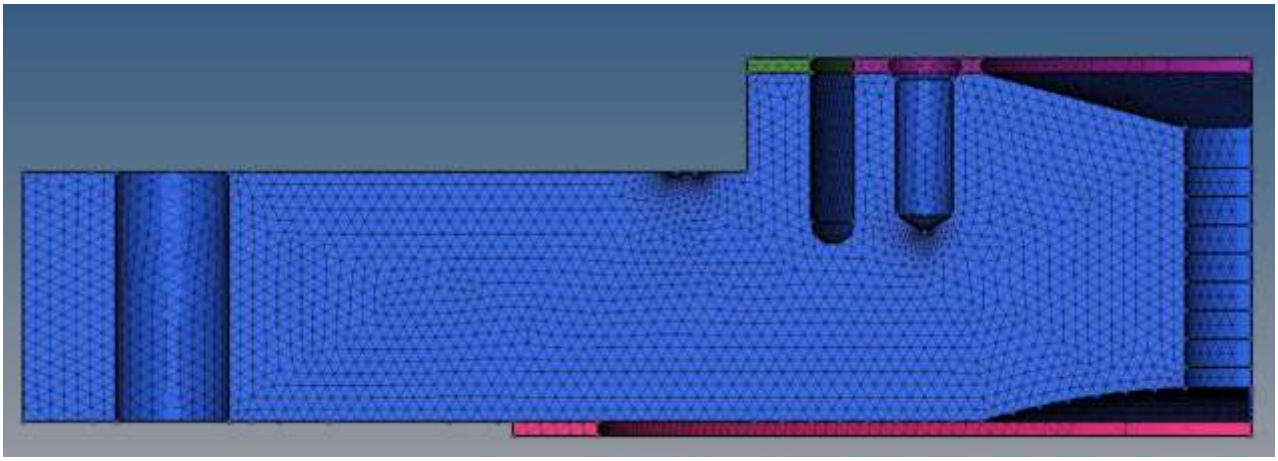

Figure 30 Injector Body Mesh Side View

The following table shows the loads applied to the injector body:

Table 5 Injector Body Loading Conditions

Pictures	Load	Value
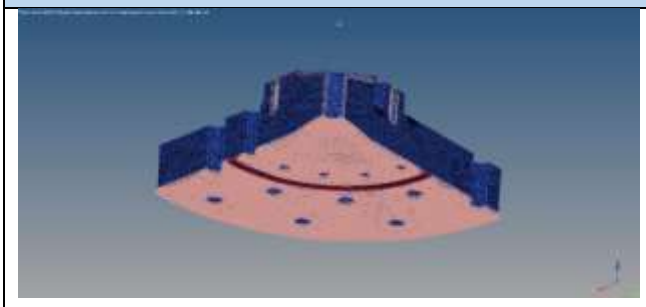	Temperature SPC	1700 °F
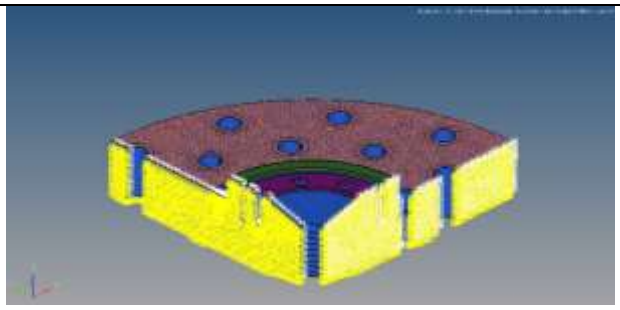	Quarter Symmetry SPC	N/A

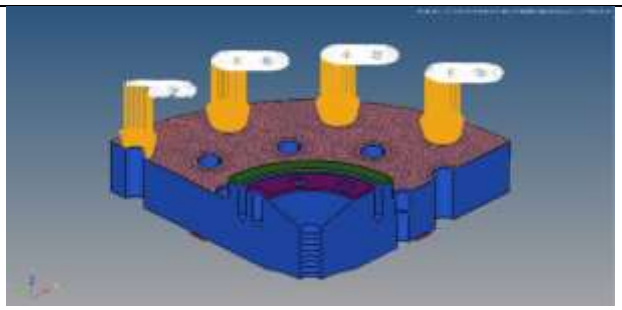	Outer Bolt Preload	10900 lbf
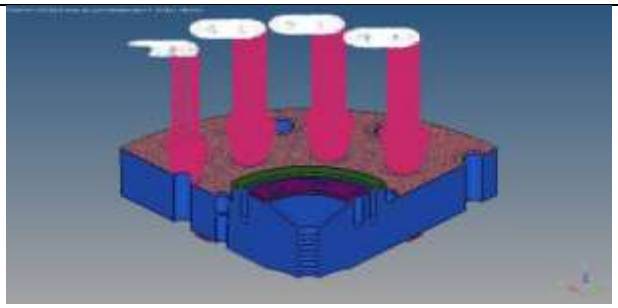	Chamber Bolt Preload	28500 lbf
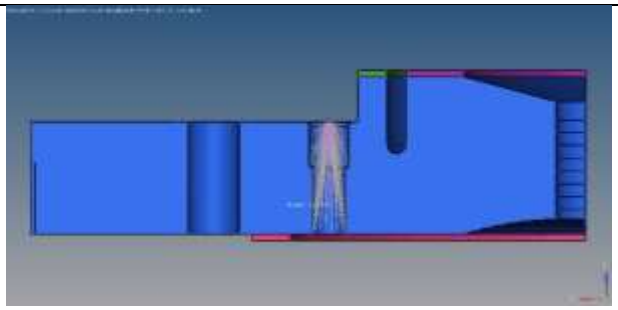	Acoustic Cavities	33 psi
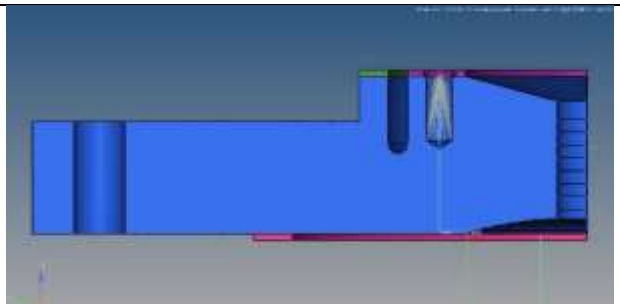	Pintle Post Preload	1230 lbf
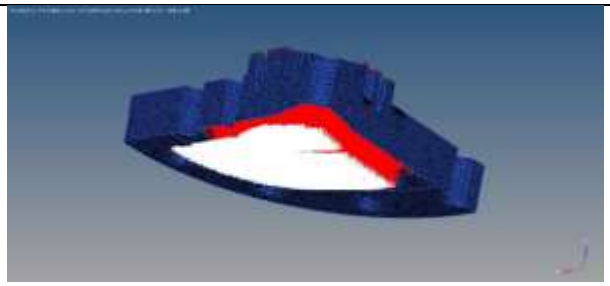	Chamber Pressure	230 psi

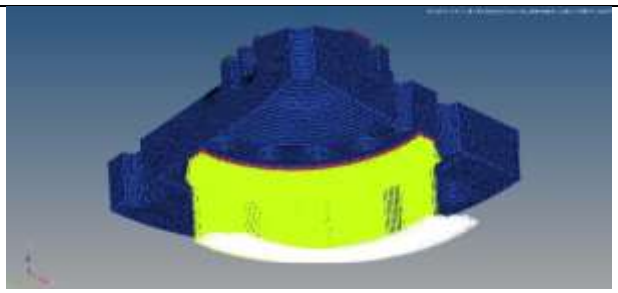	Chamber GORE Seal Pressure	3000 psi
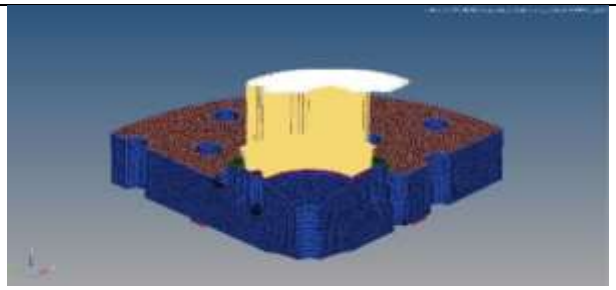	Inner GORE Seal Pressure	3750 psi
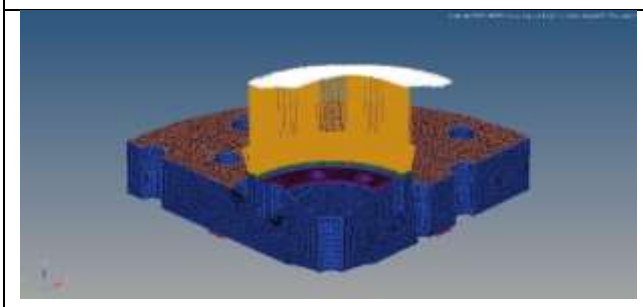	Outer GORE Seal Pressure	3750 psi
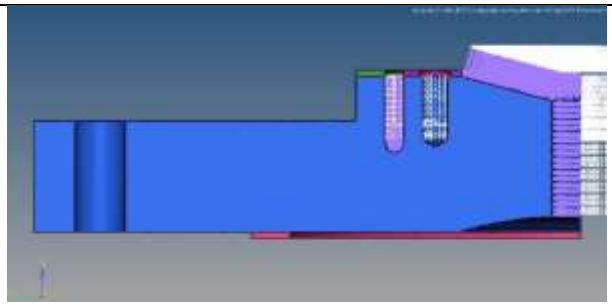	Pintle Pressure	235 psi

Once the setup was completed for the injector body, the model was run to obtain the stress analysis of the component. The vonMisses stresses were examined to determine if the injector met the desired structural requirements. The results of the FEA and the values of the vonMisses stresses experienced by the injector body are presented below.

Figure 31 reflects the stresses experienced by the critical parts mentioned above. From the overall figure we found the vonMisses stress on the outer bolted connection that goes to the structure and the acoustic cavity holes are the ones that experience a higher stress of 48840 psi which is less than the Inconel 625 yield strength of 120000 at 1800 °F. The greatest issue we encountered with the first iterations is that the part was to thin and hence it experienced more than the allowable stress. We had to modify the part by enlarging its thickness. This modification led to other ones, i.e. bolts had to be changed in size and the acoustic cavity holes had to change its dimensions in order to keep the desired dampening.

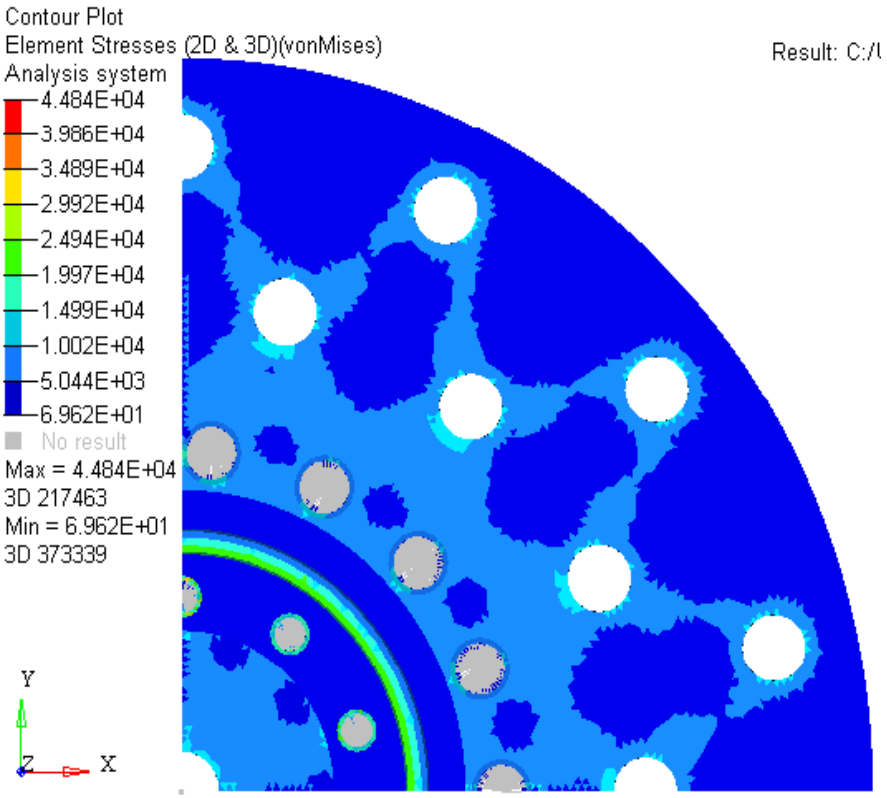

Figure 31 Injector Body Stress Contours

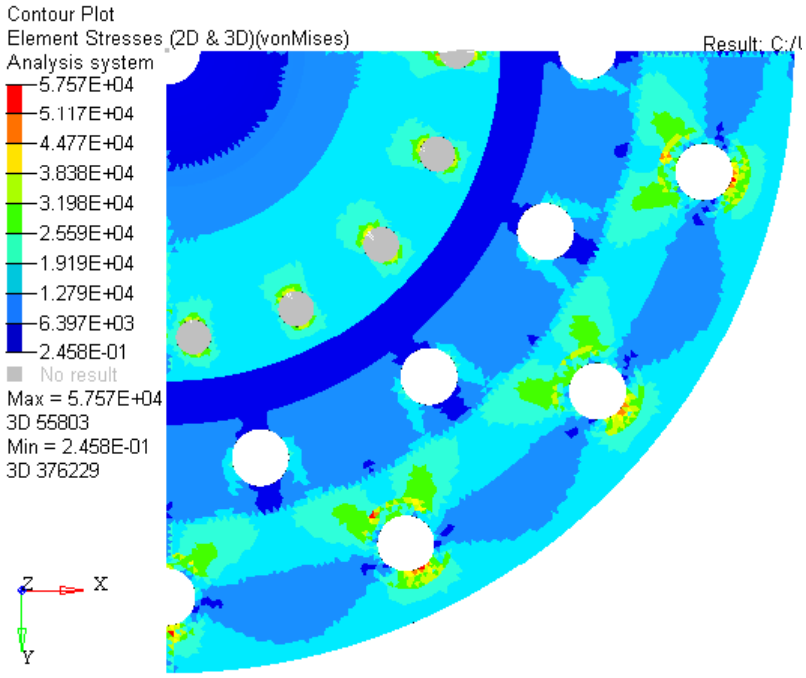

Figure 32 Injector Body Thermal Gradient

In Figure 32 we applied a thermal gradient (2160R-1080R) on injector face, convection on flange, and cryo-temperatures in cooling manifold. The highest stress is 57570 psi, less than Inconel 625 yield strength of 120000 at 1800 °F. Through this analysis we have tested and proven that the injector body will be able to safely resist the combustion temperatures without experiencing critical stresses that would endanger the engine and DEADALUS mission.

6.3 Pintle Manifold

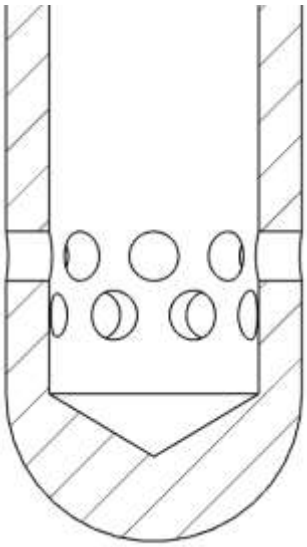

Figure 33 Pintle Primary and Secondary Holes

The pintle consists of a metal tube with a series of holes or slots close to the tip in which the propellant flows down and injects the propellant radially. The geometry of the pintle manifold can be observed in Figure 33. While the other propellant leaves the manifold though an annular gap creating an axial concentric sheet around the base of the pintle. Mixing and atomization of the propellants result from the collision between the radial jets and the annular sheet (Yang, Habiballah, Hulka, & Popp, 2004). It will have a non-permanent sealed interface between the plate and the injector body. Plumping must be welded onto component to prevent leaking and a ratio skip distance to pintle diameter between 0.8-1.5 must be met to avoid frictional losses of axial flow and flow impingement on face plate. To achieve proper mixing, secondary holes were added downstream 0.08” of post between primary radial holes.

This component must distribute the propellants into the method of injection. The material selected for the pintle manifold was Inconel 625 due to its strength properties discussed before and weldability to other like components. The first design had a port for the igniter before changing the igniter placement and to a LOX centered design.

Figure 34 Pintle Manifold First Iteration (Fuel Centered)

Figure 35 shows the new pintle design, we went for a welded design and LOX centered adjusting the pintle hole dimensions.

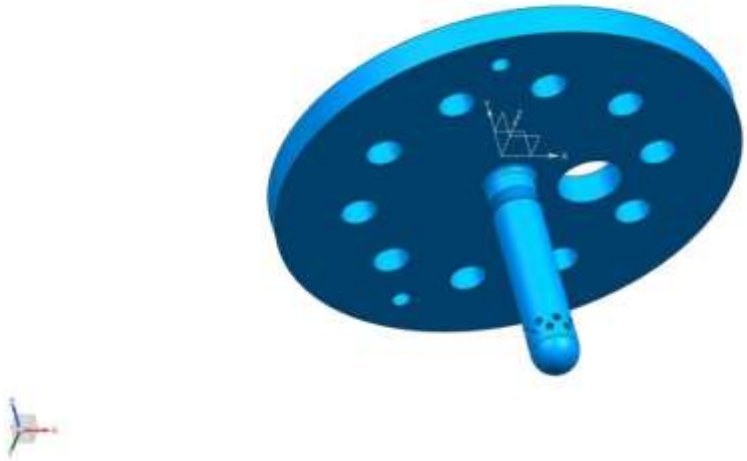

Figure 35 Pintle Manifold Geometry

The pintle must not interfere with acoustic instability tubes and allow for assembly accordingly. The ratio between the momentums of the radial and axial streams is called total

momentum ratio (TMR). Experience shows that a total momentum ratio near 45° provides optimal performance (Yang, Habiballah, Hulka, & Popp, 2004). A TMR between 0.5 and 0.8 must be met. The atomization of the spray will be verified with a high-speed camera to determine the performance of the pintle injector.

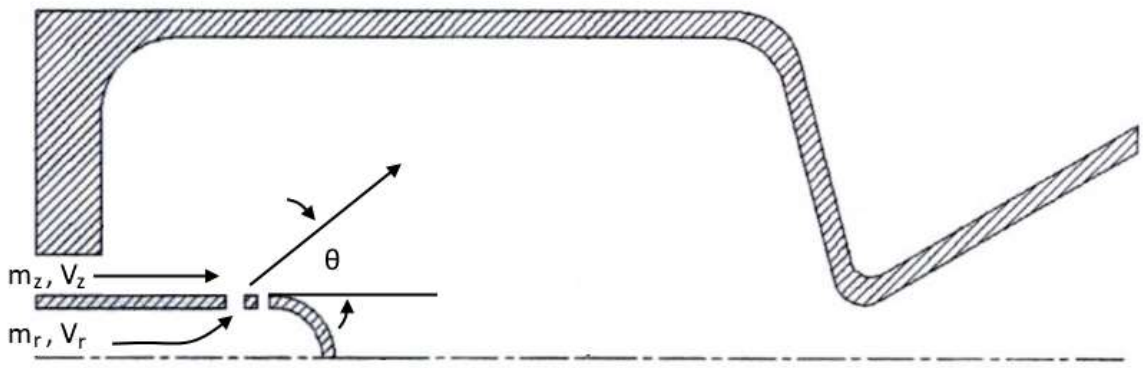

Figure 36 Pintle Injector Streams Angular Relation

No structural failure should occur i.e. plastic deformation of bolts, pintle post melting, pintle tip melting, or pressure induced stress cracks. The pintle manifold must withstand a maximum pressure condition line pressure of 400 psi, for both LOX and LCH4.

With these specifications a computer model was created in order to proceed with a finite element analysis. For the pintle manifold, the fix top surface of the bolts and the GORE seal pressure had to be specified in the program in order to apply the appropriate loads and obtain an accurate final element analysis displayed in Figure 37:

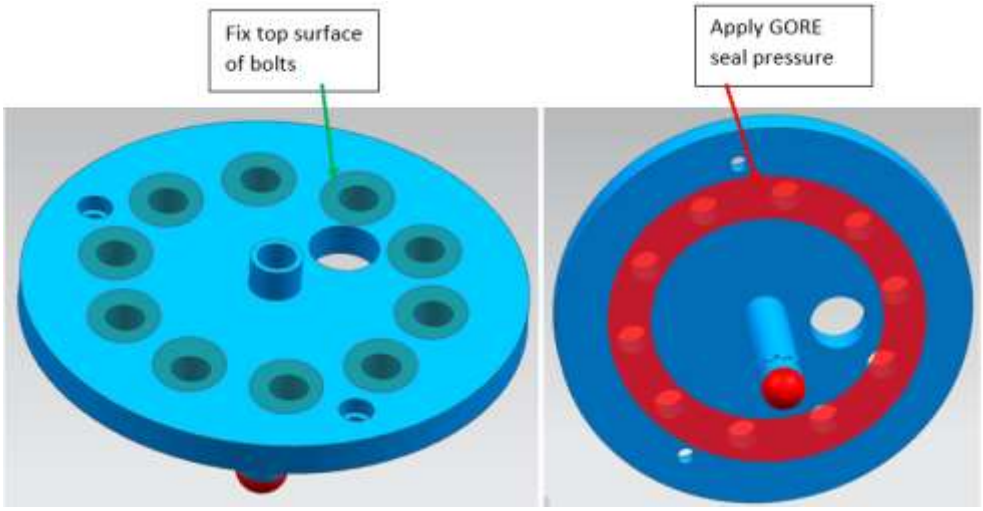

Figure 37 Bolt Area (left) GORE seal Area (right)

The Gore seal pressure will be of 2500 psi. A 400 psi pressure will be experienced from the inside of the pintle post which is the pressure at which the methane will reach the pintle once it is released from the tanks.

In order to begin the study of this component, we found the bolt preloads on the manifold using Equation 7:

$$F_c = A_c * P_g \qquad \textit{Equation 8}$$

Where:

F_c: force required to seal

A_c: compressed contact area

P_g: required GORE Seal pressure

A total preload of 2460 lbf per bolt is required to seal using 10 UNC (1/4)-20 (see Appendix).

We can also take advantage of the pintle manifold's geometry using quarter symmetry to reduce the domain by a factor of 4. The reduction in analysis domain could mean a finer mesh that can be used in the reduced analysis domain yielding more accurate results. The reduction in

computational time also plays an important role in the analysis. A mesh was created using Hypermesh 3D elements with a minimum element size of 0.02 in.

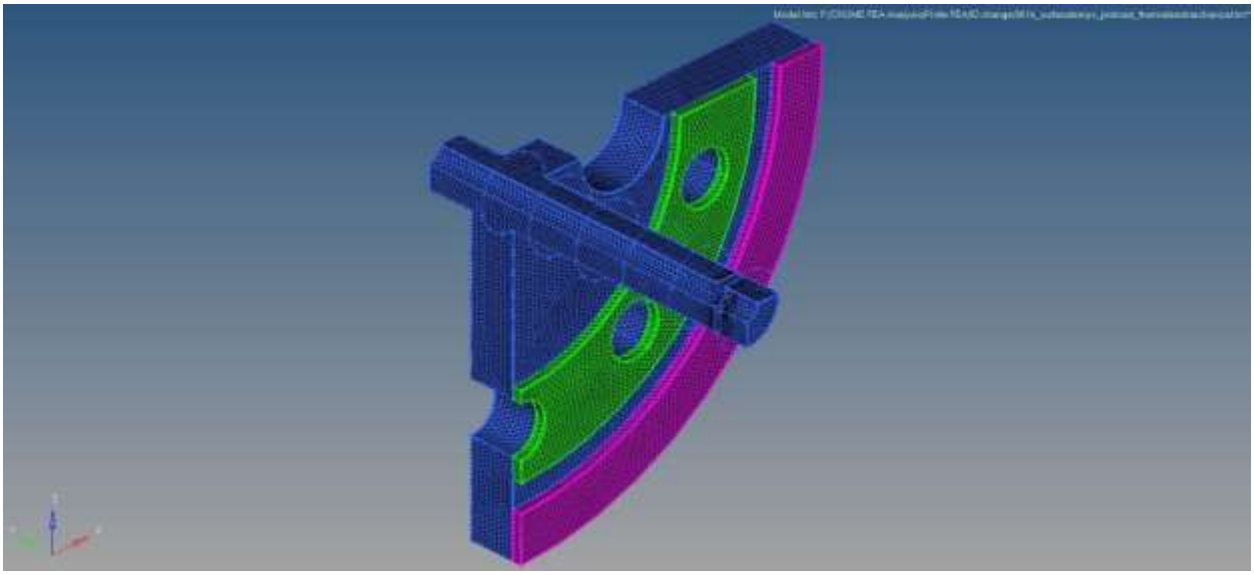

Figure 38 Pintle Manifold Mesh

The following table shows the loads applied to the pintle manifold:

Table 6 Pintle Manifold Loading Conditions

Pictures	Load	Value
	Quarter Symmetry SPC	N/A

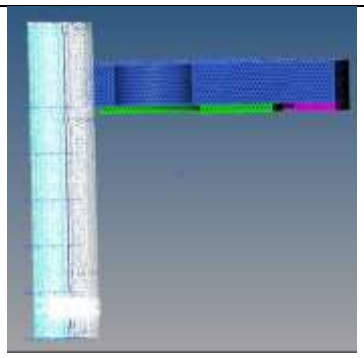	Inner Pressure	400 psi
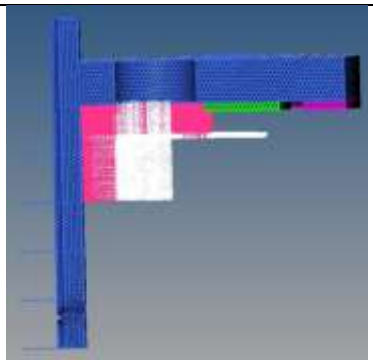	Flange Pressure	400 psi
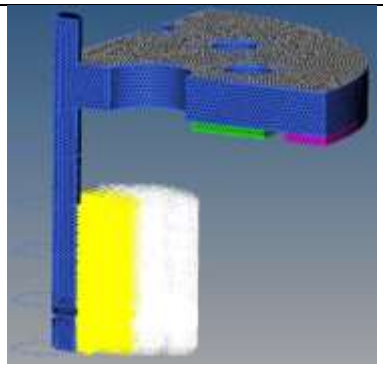	Chamber Pressure	700 psi
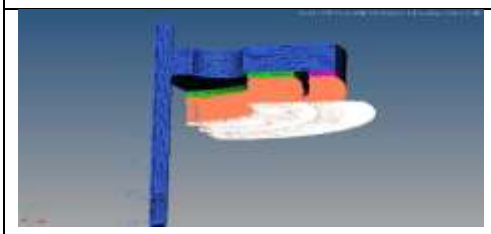	Seal Pressure	3750 psi

This is the thinnest part in the whole engine design and because of it the team took caution when designing it. When performing the initial FEA on the part, we noticed that the pintle manifold

experienced high stress levels that could compromise the design. Because of this, we changed the area of the holes to try to lower the high stress level at this area.

In Figure 39 we applied a thermal gradient (2160R-260R) simulating cryogenic temperatures from the liquid oxygen and combustion temperatures from combustion. The areas that experienced the highest stress of 40690 psi are between the series of holes. This stress is less than Inconel 625 yield strength of 120000 at 1800 °F.

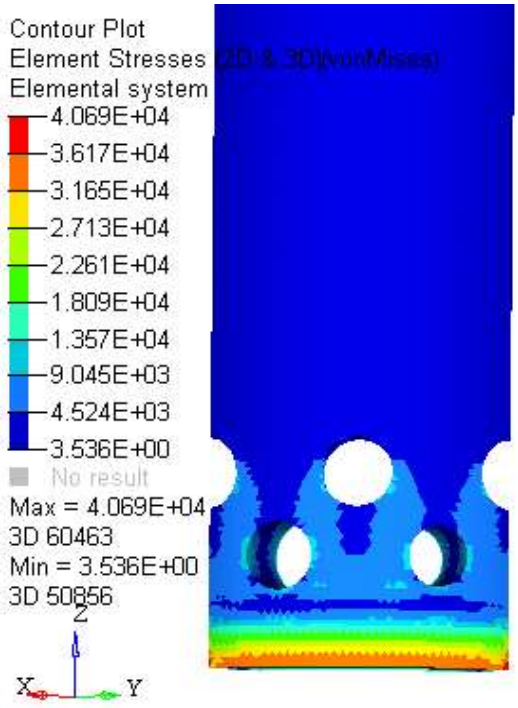

Figure 39 Pintle Manifold Thermal Gradient

The interchangeability of components allows to take into consideration that instead of using the two arrays of holes at the end of the injector other shapes, like slots, could be tested with different patterns.

Chapter 7: Valves & Instrumentation

Different valve types were considered for this engine. Precise control of the propellant going into the engine is crucial for the operation of CROME. Because of this, throttle valves selection is crucial for the succes of the mission. Two main valves will be controlling the flow from 125 to 500 lbf to vary the thrust for vehicle dynamic control. Following advice from JSC, and setting the requirement needed for each throttle level, we decided to use ball valves because they only require a quarter turn to be completely opened or closed. Although ball valves have poor throttling characteristics because in a throttling position, the partially exposed seat may be prone to erosion as a result of high velocity flows, we decided to use a ball valve with a v-shaped port. This allows a better control through the position of the valve. The minimum required flow coefficient (Cv) was obtained from the valve requirements. This indicated valve performance, the larger the Cv, the smaller pressure drop caused by the valve. The equation for C_v is as follows:

$$C_v = Q\sqrt{\frac{SG}{\Delta P_V}} \qquad \textit{Equation 9}$$

Wehre:

Q: volumetric flow ratethrough the valve (Gal/min)

SG: specific gravity of the fluid

ΔP_v: pressure drop across the valve

Based on the valve requirements, it was determined that the valve would require a minimum C_v of 15.

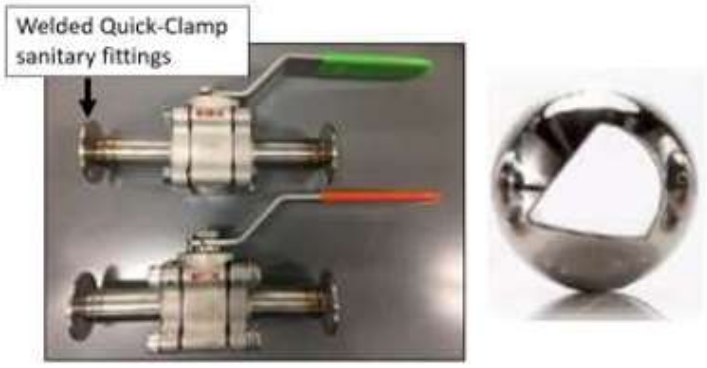

Figure 40 Habonim Ball Valves (left) 60° v-port (right)

The valves were manufactured by Habonim Induatrial Valve & Actuators and provided a 60° v-port ball valve which met the control and pressure drop requirements for our system. An actuator was also selected based on the specification of the valves as wel as CROME's control requirements. The maximum valve reaction time from fully closed to fully open is 0.5 s. Based on these requirements a DC motor was selected as the actuator for the valves combined with a 71:1 gear ratio gearbox. The minimum operating temperature for the gear box is -22 °F and since we operate at cryogenic temperatures, a connector was designed to act as a thermal standoff and also transfer the required torque from the gearbox to the valve. Computational analysis was done to ensure the integrity of the connector. The material selected for this connector was titanium alloy Ti-64 due to its high strength and low thermal conductivity. Also, this connector will be 3D printed at the W.M. Keck Center at UTEP. Figure 41 shows the temperature contours.

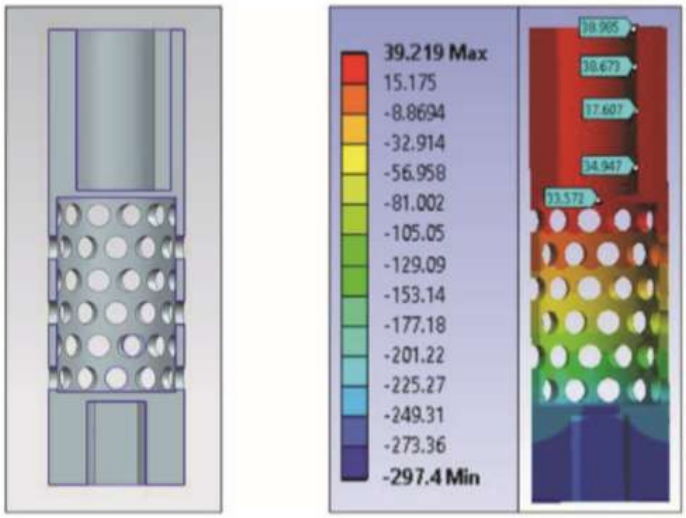

Figure 41 Connector & Thermal Contour

A complete assebly of the valve and the connector is shown in Figure 42:

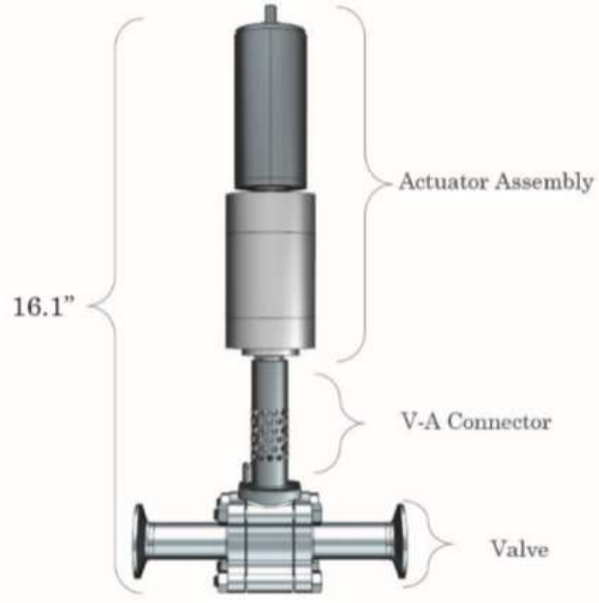

Figure 42 Valve-Actuator Assembly

To measure all the electrical phenomenon such as voltage, current, temperature, and pressure. A Data Acquisition System (DAQ) was developed. The design development are discussed in detail in the thesis written by Javier Chaparro. For the selection of instrumentation we

closely worked with the DAQ system team in order to comply with the voltage requierements. Nonetheless, the DAQ system is capable to support more than the required instrumentation in case the team ever needs to include other data parameters. All the data will be recorded using LabView Software. One of the main reasons the team decided to use LabView is that with its current capibilities we are able to measure real time data like pressure, temperature, etc. Table 5 shows the rest of the valves and instrumention that will be used:

Table 7 DEADALUS Instrumentation

Picture	Part	Number Required	Vendor
	Static Pressure Transducer	16	Omega
	Pressure Transducer External Amplifier	16	Omega
 f 	Dynamic Pressure Transducer	2	PCB Piezotronics

	8-Channel Signal Conditioner	1	Omega
	Thermocouples	32	Omega
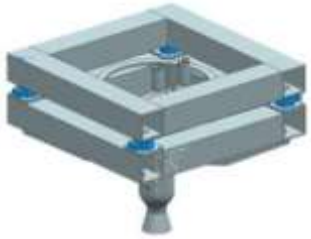	Load Cell	4	
	Load Cell External Amplifier	3	Omega
	Accelerometer	2	Omega
	Accelerometer Power Supply	2	Omega

	Turbine Flow Meters	4	Hoffer Flow Controls
	Flow Meter Signal Conditioner	4	Hoffer Flow Controls
	Control Motors	2	Maxon Motors
	Igniter Spark Pug	2	
	Indicator Lights	3	McMaster Carr
	Buzzer	1	McMaster Carr
	Solenoid Valves	8	ASCO
	Relief Valves	2	Swagelok

	Check Valves	4	Swagelok
	Hand Valves	4	Swagelok
	Line Connections		Swagelok
	Pressure Gauge	2	Omega
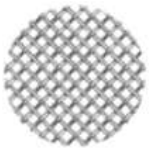	Filter	4	Norman Filters
	Pressure Regulators	8	Airgas

Chapter 8: Future Work

The CROME and DEADALUS has been in production since 2015. At the beginning of the project the vehicle requirements were defined per the purpose of the mission. Once all the requirements were set, the the design process started. The engine parts were built in CAD models and FEA were performed on them. Various iterations were done until an optimal design was achieved which met the previously established requirements. During this process the blueprints for the engine were constantly changing to meet the requirements of the project. A Geometric Dimensioning and Tolerancing (GD&T) format was used throughout the project to keep track of all the drawing under the same format. Once the FEA returned optimal results and the blueprints for the parts were finished, the design was approved.

After this, the drawings were sent to a local company in El Paso, TX for a quote to build it. Unfortunately, the local company had to send some of the parts to another company since due to the material and the difficulty degree of the parts it was not possible to make them so it was given to another manufacturer. This added lag time to the overall project. Once it was finished and built it was sent back to the cSETR and all of this process happened while this thesis was in development.

Figure 43 Rendering of cSETR's tRIAc

The hot fire test procedure is being written and will be submitted for approval. It is expected that for the year 2018 the actual hot fire tests will be conducted now that the Technology Research and Innovation Accelerration Park (tRIAc) has been completed. Water test setup procedure has been approved and it is ready for actual testing since the

injetor has been manufactured. This test will verify the the design requirements, principles and performance have been met. In the test, the actual flowrate vs pressure drop will be measured. Once the results are obtained they will be compared to the calculated theoretical values and accroding to the comparisons corralations can be adjusted. With this test, the spray angle and injection stream quality can be visually examined. As the name of the test suggests, a water pump will deliver water to the injector which then will spray the water into a container with clear acrylic windows which will allow the inspection of the spray. The setup can be seen in Figure 44:

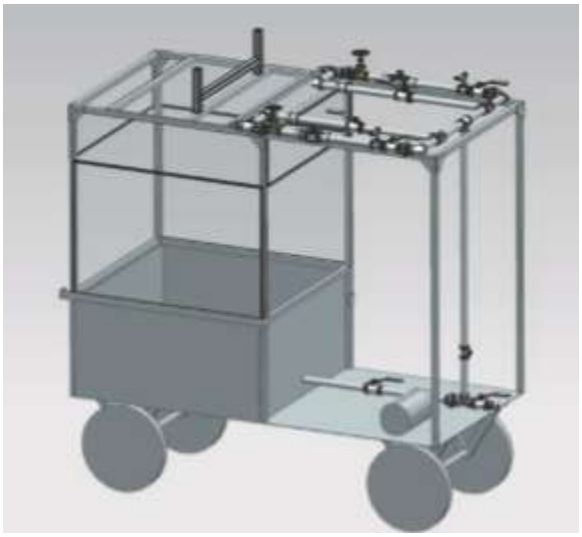

Figure 44 Water Test Setup

This test will be performed on tRIAc at Fabens, TX. This new location and facilities were built and chosen since UTEP no longer has the facilities to support the test of such big engines without putting in hazard the university and its students and faculty. Also, this new facility, will promote and enhance the partenership the university holds with NASA in order to promote the development of space technologies. The test procedure has been aproved and now that the injector has been built another team can test and continue the work.

Chapter 9: Conclusion

This project was based on NASA's Morpheus vehicle in order to design and create the CROME engine for the DEADALUS vehicle. The requirements for this engine was the usage of LO2-LCH4 propellants and a thrust of 500 lbf. The engine was fully assembled during the completion of this document. The process of design and analysis of its components were described in the above sections of this thesis. The objective of this project is to successfully perform a hot fire test at the tRIAC test facility. Aerospace industry has been growing rapidly in the past decades, the study of LOX/LCH4 capabilities will help future aerospace endeavors more affordable.

References

Atyam, D. M., & Hguyen, N. H. (2015). *Designing and Testing Liquid Engine for Additive Manufacturing.* Orlando, FL: 51st AIAA/SAE/ASEE Joint Propulsion Conference.

Brown, C. D. (1996). *Spacecraft Propulsion.* Washington D.C.: American Institute of Aeronautics and Astronautics.

Budynas, R. G., & Nisbett, K. J. (2003). *Shingley's Mehcanical Engineering Design.* New York, NY: McGraw-Hill.

Candelaria, J. (2017). *Theoretical Acoustic Absorber Design Approach for LOX/LCH4 Pintle Injector Rocket Engines.* El Paso, TX: UTEP Center for Space Exploration and Techonology Research.

Douglass, H. W., Combs, L. P., & Keller, R. B. (1975). *Liquid Rocket Engine Combustion Stabiliztion Devices.* Washington, D.C.: National Aeronautics and Space Administration.

Dressler, G. A., & Bauer, M. J. (2000). TRW Pintle Engine Heritage and Performance Characteristics. *36th AIAA/ASME/SAE/ASEE Joint Propulsion Conference and Exhibit*.

Gill, G. S., Nurick, W. H., Keller, R. B., & Douglass, H. W. (1976). *Liquid Rocket Engine Injectors.* Cleveland, OH: National Aeronautics and Space Administration.

Hart, J., & Devolites, J. (2014). *Morpheus Vertical Test Bed Flight Testing.* Big Sky , MT: IEEE Aerospace Conference.

Huzel, D. K., & Huang, D. H. (1992). *Modern Engineering for Design of Liquid-Propellant Rocket Engines.* Washington D.C.: American Institue of Aeronautics and Astronautics.

Lopez, I. (2017). *Design of a 2000 lbf LOX/LCH4 Throttleable Rocket Engine for a Vertical Lander.* El Paso, TX: UTEP Center for Space Exploration and Techonology Research.

Sutton, G. (2001). *Rocket Propulsion Elements.* New York: Wiley.

Sutton, G. P., & Biblarz, O. (2010). *Rocket Propulsion Elements.* Hoboken, NJ: John Wiley & Sons.

Trillo, J. E. (2016). *Design of a 500 lbf Liquid Oxygen and Liquid Methane Rocket Engine for Suborbital Flight.* El Paso, TX: UTEP Center for Space Exploration and Technology Research.

Yang, V., Habiballah, M., Hulka, J., & Popp, M. (2004). *Liquid Rocket Thrust Chambers: Aspects of Modeling, Analysis, and Design.* Reston, VA: American Institue of Aeronautics and Astronomics.

Appendix

A1 Thrust chamber wall thickness analysis

$$\sigma_h = \frac{P_c(d_i + t)}{t * 2} = \frac{700(3.5 + 0.25)}{0.25 * 2} = 5250\ psi$$

Where:

σ_h: Hoop stress

P_c: maximum chamber pressure

d_i: inner diameter of the chamber

t: wall thickness

$$\sigma_l = \frac{P_c * d_i}{\sigma_h * 4} = \frac{700 * 3.5}{5250 * 4} = 2450\ psi$$

Where:

σ_l: longitudinal stress

P_c: maximum chamber pressure

d_i: inner diameter of the chamber

$$\sigma_v = \sqrt{\sigma_h^2 + \sigma_l^2 + (\sigma_h * \sigma_l)} = \sqrt{5250^2 + 2450^2 + (5250 * 2450)} = 6813.77\ psi$$

Where:

σ_v: vonMisses stress

σ_h: Hoop stress

σ_l: longitudinal stress

$$S.F. = \frac{S_y}{\sigma_v} = \frac{11750}{6813.77} = 1.72$$

Where:

S.F.: Safety Factor

S_y: Inconel 718 yield strength @ 2000 °F

σ_v: vonMises stress

Thickness of wall (in)	Hoop Stress (psi)	Longitudinal Stress (psi)	Vonmises Stress (psi)	S.F
0.14	9100	4375	11906.43209	0.986861548
0.15	8516.666667	4083.333333	11134.79282	1.055250887
0.16	8006.25	3828.125	10459.61308	1.123368513
0.17	7555.882353	3602.941176	9863.870584	1.191215953
0.18	7155.555556	3402.777778	9334.325757	1.258794722
0.19	6797.368421	3223.684211	8860.526316	1.326106326
0.2	6475	3062.5	8434.11043	1.393152259
0.21	6183.333333	2916.666667	8048.309001	1.459934006
0.22	5918.181818	2784.090909	7697.583674	1.52645304
0.23	5676.086957	2663.043478	7377.359287	1.592710825
0.24	5454.166667	2552.083333	7083.823206	1.658708816
0.25	5250	2450	6813.772817	1.724448454
0.26	5061.538462	2355.769231	6564.498216	1.789931174
0.27	4887.037037	2268.518519	6333.690969	1.855158399
0.28	4725	2187.5	6119.372415	1.920131544
0.29	4574.137931	2112.068966	5919.836813	1.98485201

A2 Injector Body/Chamber Flange Bolt Analysis

$$P = P_c * A_{cc} = 700 * 15.6 = 10920\ psi$$

Where:

P: total pressure

P_c: maximum chamber pressure

A_{cc}: chamber contact area

$$A_c = k_1 * A_s = 1.2 * 5.86 = 7.03\ in^2$$

Where:

A_c: compressed contact area

k_1: compressibility factor given by manufacturer

A_s: uncompressed contact area of the GORE seal

$$F_c = \left(A_c * P_g\right) + P = (7.03 * 2500) + 10920 = 28503\ psi$$

Where:

F_c: total force needed to seal

A_c: compressed contact area

P_g: required GORE seal pressure

P: total pressure

$$F_s = \frac{F_c}{N} = \frac{28503}{14} = 2035.93\ lbf$$

Where:

F_s: force required per bolt to seal

F_c: total force needed to seal

N: number of bolts

$$F_i = F_s * n_s = 2034.93 * 1.2 = 2443.11\ lbf$$

Where:

F_i: preload on the bolts

F_s: force required per bolt to seal

n_s: sealing factor (ratio between the preload on the bolts and the required force per bolt to seal)

A3 Manifold Cap Bolt Analysis

$$A_c = k_1 * A_s = 1.2 * 5.47 = 6.56\ in^2$$

Where:

A_c: compressed contact area

k_1: compressibility factor given by manufacturer

A_s: normal contact area (uncompressed)

$$F_c = A_c * P_g = 6.56 * 2500 = 16401\ lbf$$

Where:

F_c: force required to seal

A_c: compressed contact area

P_g: required GORE seal pressure

$$F_s = \frac{F_c}{N} = \frac{16401}{10} = 1640.1\ lbf$$

Where:

F_s: required force per bolt to seal

F_c: total force needed to seal

N: number of bolts

$$F_i = F_s * n_s = 1640.1 * 1.2 = 2460.15\ lbf$$

Where:

F_i: preload on the bolts

F_s: required force per bolt to seal

n_s: sealing factor (ratio between the preload on the bolts and the required force per bolt to seal)

Vita

Daniel Vargas Franco obtained his Bachelor of Science degree in Mechanical Engineering from the University of Texas at El Paso in the spring of 2015. He started working in the cSETR in fall 2014 and after his undergraduate studies, he pursued his Master's degree in Mechanical Engineering to continue his research in LOX/LCH4 technologies. During his graduate studies, he was selected as a Pathways Intern at NASA Kennedy Space Center to work with the Environmental and Life Support Systems branch developing ground support equipment for Space Launch System (SLS) and the Orion spacecraft.

Contact Information: danyvancouver7@gmail.com

This thesis was typed by Daniel Vargas Franco